

**A SIMULATION STUDY OF PHOTOVOLTAIC THERMAL USING PHASE
CHANGE MATERIAL**

AHMAD SYAHIR BIN MUHAMMAD IBRAHIM

**A project report submitted in fulfilment of the requirements for the degree of
Bachelor of Mechanical Engineering (Hons.)**



UNIVERSITI TEKNIKAL MALAYSIA MELAKA

JANUARY 2022

DECLARATION

I hereby declare that this project report entitled “**A Simulation Study of Photovoltaic Thermal Using Phase Change Material**” is based on my original work except for citations and quotations which have been duly acknowledged.

Signature

Syahir

Name

AHMAD SYAHIR BIN MUHAMMAD IBRAHIM

Date

9th JANUARY 2022

اونيورسيتي تيكنيكل مليسيا ملاك

UNIVERSITI TEKNIKAL MALAYSIA MELAKA

APPROVAL

I hereby declare that I have read this project report entitled “**A Simulation Study of Photovoltaic Thermal Using Phase Change Material**” and in my opinion this report is sufficient in terms of scope and quality for the award of the degree of Bachelor of Mechanical Engineering (Hons.).

Signature

:

Supervisor's Name

:

Date

:



DEDICATION

To my beloved mother and father, and myself.



ABSTRACT

Photovoltaic thermal (PVT) systems have arisen as a critical study topic in recent years, owing to the world's growing energy need. Phase change materials (PCMs) are regarded as the optimal materials for efficiently harvesting thermal energy from renewable energy sources. However, today's PCMs have a significant disadvantage in terms of thermal conductivity. Over the last several years, there has been an upsurge in study targeted at fixing the issue. Thermal conductivity increases the amount of heat stored and extracted during the melting and solidification processes. Besides, parameters such as the thickness of the PCM, the types of PCM, and the effect of the melting temperature can also affect the performance of the PVT/PCM system. Hence, a simulation study using ANSYS FLUENT has been done to investigate the effect of thickness and properties of PCM for weather conditions in Malaysia. The best PCM types and thickness for this model are also selected. The thermal and electrical efficiency of the system is also studied in this report. Based on the results, Lauric Acid has the best thermal and electrical efficiency when PCM thickness increases. An optimum thickness of 30 mm is selected for Lauric Acid as it shows the best results compared to all other PCMs in this study.

ACKNOWLEDGEMENTS

To begin, I would like to offer my heartfelt appreciation to my supervisor, Dr. Mohd. Afzanizam bin Mohd. Rosli, of the Faculty of Mechanical Engineering at Universiti Teknikal Malaysia Melaka (UTeM), for his critical supervision, support, and encouragement in completing this project report.

I would want to express my gratitude to all of my friends, my mother, Mrs. Afifah, my father, Mr. Muhammad Ibrahim, and Ms. Nur Adlin Fadhlina for their moral support in obtaining this degree. Additionally, I'd want to express my gratitude to everyone who was there throughout critical stages of the project's execution.

Finally, I would also like to thank myself for all of the effort put into this study and never giving up until the research is finished.

UNIVERSITI TEKNIKAL MALAYSIA MELAKA

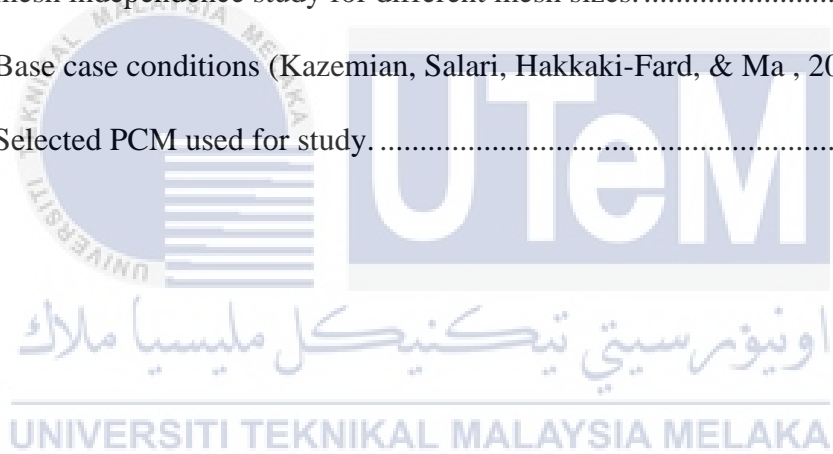
TABLE OF CONTENTS

DECLARATION	i
APPROVAL	ii
DEDICATION	iii
ABSTRACT	iv
ACKNOWLEDGEMENTS	v
LIST OF TABLES	viii
LIST OF FIGURES	ix
LIST OF SYMBOLS / ABBREVIATIONS	xii
CHAPTER	1
1.INTRODUCTION	1
1.1 BACKGORUND	1
1.2 PROBLEM STATEMENT.....	3
1.3 OBJECTIVE.....	4
1.4 SCOPE OF PROJECT	4
2. LITERATURE REVIEW	5
2.1 INTRODUCTION	5
2.2 OVERVIEW OF PVT/PCM SYSTEM	5
2.3 PHASE CHANGE MATERIAL	7
2.3.1 CLASSIFICATION OF PHASE CHANGE MATERIAL.....	8
2.3.2 SELECTION CRITERIA FOR PHASE CHANGE MATERIAL	10
2.4 EFFECT OF THICKNESS OF PCM IN PVT/PCM SYSTEM	11
2.5 EFFECT OF PROPERTIES OF PCM IN PVT/PCM SYSTEM.....	14
2.5.1 THE EFFECT OF MELTING TEMPERATURE OF THE PCM	14
2.5.3 EFFECT OF THERMAL CONDUCTIVITY TO THE PVT/PCM SYSTEM ..	17
2.6 PREVIOUS STUDIES ABOUT PVT/PCM SYSTEM.....	21

2.7	MODEL COMPARISON	23
3.	METHODOLOGY	28
3.1	INTRODUCTION	28
3.2	METHODOLOGY CHART	28
3.3	SIMULATION PROCEDURE.....	30
3.3.1	SIMULATION SETUP	30
3.3.2	INITIAL AND BOUNDARY CONDITIONS.....	32
3.3.3	FLUID FLOW FEATURES AND SIMULATION ASSUMPTIONS	33
3.3.4	GOVERNING EQUATIONS	34
3.3.5	NUMERICAL METHOD	37
3.3.6	MESHING.....	38
3.4	THERMODYNAMIC ANALYSIS.....	40
4.	RESULTS AND DISCUSSION.....	42
4.1	VALIDATION.....	42
4.1.1	QUANTITATIVE VALIDATION RESULTS	42
4.1.2	QUALITATIVE VALIDATION RESULTS	44
4.2	PROPOSED RESULT.....	48
4.2.1	SELECTION OF PCM.....	48
4.2.2	SIMULATION STUDY OF USING DIFFERENT THICKNESS OF PCM ...	54
5.	CONCLUSION AND RECOMMENDATION FOR FUTURE WORK.....	59
5.1	CONCLUSION.....	59
5.2	RECOMMENDATIONS FOR FUTURE WORK	60

LIST OF TABLES

Table 2.1 - Desired properties of PCM.....	11
Table 2.2 - Example of types and properties of PCM used in previous studies.....	19
Table 2.3 - model comparison of previous studies.....	23
Table 3.1 - PVT/PCM system model dimension (Kazemian, Salari, Hakkaki-Fard, & Ma , 2019).....	30
Table 3.2 - mesh independence study for different mesh sizes.....	39
Table 4.1 - Base case conditions (Kazemian, Salari, Hakkaki-Fard, & Ma , 2019).....	42
Table 4.2 - Selected PCM used for study.....	49



LIST OF FIGURES

Figure 2.1- classification of PCMs (Reji Kumar, Samykano, Pandey , Kadirgama, & Tyagi, 2020).....	9
Figure 2.2 - thermal energy output with varying PCM thickness (Su, Jia, Lin, & Fang , 2017).	12
Figure 2.3 - electrical energy output for varying PCM thickness (Su, Jia, Lin, & Fang , 2017).	12
Figure 2.4 - effect of PCM thickness to the performance of PVT (Malvi, Dixon-Hardy, & Crook, 2011).....	13
Figure 2.5 - effect of solar radiation to the melted PCM (Kazemian, Salari, Hakkaki-Fard, & Ma , 2019).	15
Figure 2.6 - electrical efficiency for different melting point (Su, Jia, Lin, & Fang , 2017).16	16
Figure 2.7 - thermal energy output for varying melting point (Su, Jia, Lin, & Fang , 2017).	16
Figure 2.8 - effect of thermal conductivity to different parameter to PCM (Kazemian, Salari, Hakkaki-Fard, & Ma , 2019).	17
Figure 2.9 - schematic diagram of (a) PVT, and (b) PVT/PCM.	24
Figure 2.10 - schematic diagram of the simulation model.	25
Figure 2.11 - schematic diagram of PVT collector with PCM.....	26
Figure 2.12 - sectional view of the PVT collector with PCM.	26
Figure 2.13 - schematic diagram of PVT collector with PCM.....	27
Figure 3.1 - flow chart of methodology of the project.	29

Figure 3.2 - isometric view of the model.	31
Figure 3.3 - schematic diagram of the reference model (Kazemian, Salari, Hakkaki-Fard, & Ma , 2019).	31
Figure 3.4 - boundary conditions of the present study presented in ANSYS Fluent software.	33
Figure 3.5 - meshing results produced in the present study.	38
Figure 4.1 -comparison of surface temperature of (a) created geometry (b) reference paper (Kazemian, Salari, Hakkaki-Fard, & Ma , 2019)	43
Figure 4.2 - PCM layer temperature comparison of (a) created geometry and (b) reference paper.	43
Figure 4.3 - Comparison of percentage of melted PCM between present study and numerical results of (Kazemian, Salari, Hakkaki-Fard, & Ma , 2019).....	45
Figure 4.4 - Comparison of Average surface temperature of PVT/PCM system between present study and numerical results of (Kazemian, Salari, Hakkaki-Fard, & Ma , 2019)...	46
Figure 4.5 - Comparison of Average coolant outlet temperature between present study and numerical results of (Kazemian, Salari, Hakkaki-Fard, & Ma , 2019).....	47
Figure 4.6 - Percentage of melted PCM for different types of PCM.....	50
Figure 4.7 - surface temperature of different types of PCM.	51
Figure 4.8 - Average coolant outlet temperature of different types of PCM.	52
Figure 4.9 - Comparison of electrical and thermal efficiency of PVT/PCM system with different types of PCM.	53
Figure 4.10 - thickness of PCM.....	54
Figure 4.11 - percentage of melted PCM of different thickness.	54
Figure 4.12 - surface temperature of PVT/PCM system using different thickness of PCM.	55

Figure 4.13 - average coolant outlet temperature for different thickness of PCM..... 56

Figure 4.14 - Electrical efficiency of PVT/PCM system with different thickness..... 57

Figure 4.15 – Thermal efficiency of PVT/PCM system with different thickness..... 58



LIST OF SYMBOLS / ABBREVIATIONS

A	Area, m ²
A_{mush}	Mushy zone constant
C_p	Specific heat capacity, J/kg.K
\dot{E}	Power, W
h	Enthalpy of fusion, J/kg
ΔH	Latent enthalpy, J/kg
H	Material enthalpy, J/kg
K	Thermal conductivity, W/m ² .K
\dot{m}	Mass flow rate, kg/s
P	Pressure, Pa
t	Time
T	Temperature, K
V	Velocity
α	Absorptivity
β	Liquid fraction
η	Energy efficiency, %
ε	Emissivity
ρ	Density, kg/m ³
μ	Dynamic viscosity, kg/m.s
τ	Glass cover transmissivity
eff	Effective
el	Electrical
f	Fluid

<i>g</i>	Glass cover
<i>in</i>	Inlet
<i>out</i>	Outlet
<i>PCM</i>	Phase change material
<i>PV</i>	Photovoltaic
<i>PVT</i>	Photovoltaic thermal
<i>th</i>	thermal



CHAPTER 1

INTRODUCTION

1.1 BACKGORUND

Economic growth has been accelerated by the fast rise of the human population, along with technical improvements. Overproduction of energy to meet consumer demand has led in the depletion of fossil fuels (prime source of energy generation). On the other side, human activities associated with energy generation and consumption have resulted in environmental problems such as ozone depletion and global warming, which can result in climate change. Thus, these negative environmental changes that have been wreaking havoc on the globe may be mitigated by utilizing renewable energy sources such as solar energy. Nowadays, solar energy is readily available on the market due to its abundance, pollution-free nature, and ability to be used for agricultural, residential, and commercial purposes. Although solar photovoltaic systems are expensive to construct, this technology is now widely known and has a low maintenance cost. Indeed, two of the world's greatest economies, China, and India, have already begun producing solar energy on a significant scale, making them the world's greatest solar energy producers. The solar photovoltaic panel converts solar radiation into electrical energy, while the remaining energy is absorbed or reflected by the photovoltaic module as thermal energy. (Reji Kumar, Samykano, Pandey , Kadirgama, & Tyagi, 2020).

However, the current solar photovoltaic (PV) technology has many drawbacks such as when the heat absorbed increases with time, the electrical efficiency of the solar PV panel decreases and the rest of the solar radiated into the panel is wasted as heat. This means that

when the electrical efficiency of the PV panel decreases, the electrical energy that can be generated from the PV system also decreases. As a solution, a lot of research has been made to overcome this problem such as the introduction of Photovoltaic Thermal (PVT) system, a system which combines both solar PV and solar thermal system that produce both electrical energy and heat energy at the same time. This technology has gained popularity over the years. When solar radiation is absorbed by the photovoltaic cell and converted to electrical energy, a solar thermal system integrated into the PVT system provides a cooling effect that cools the PV cells and absorbs excess heat from the PV panel whenever their temperature rises, using either air or water as the cooling fluid in the system. The PVT system considerably improves the electrical efficiency of the system by absorbing surplus heat from the photovoltaic panel using another medium such as an air collector, a water collector, or a combination of both air and water collectors that operate as a coolant for the system. (Diwania, Agrawal, Siddiqui, & Singh , 2020).

Additionally, the type of collector utilized in a PVT system is critical in decreasing the temperature of the photovoltaic panel. There are several varieties of thermal collectors available on the market, including PVT air collectors, PVT water collectors, and hybrid PVT air/water collectors are called PVT combi collectors. These thermal collectors each have their own unique method of collecting surplus heat from the photovoltaic panel, and each collector has its own set of advantages and disadvantages. For instance, PVT air collectors employ a single or double channel thermal collector and operate with air as the working fluid, whereas PVT water collectors employ a sheet and tube or roll bond absorber and operate with water as the working fluid. (Diwania, Agrawal, Siddiqui, & Singh , 2020).

Recently, the incorporation of phase change material (PCM), a substance capable of heat absorption, storage, and release, into the PVT system has been extensively investigated by individuals with varying specialties in the field of solar technology. The expansion of study

into the PCM in PVT system was anticipated owing to its properties as a high-latent heat capacity storage material capable of collecting and releasing a considerable quantity of heat energy throughout the melting and solidifying processes (Reji Kumar, Samykano, Pandey , Kadirgama, & Tyagi, 2020). When the ambient temperature exceeds the temperature of the PCM material, heat is transmitted from the environment to the substance, which transforms to a liquid state. When the ambient temperature is lower than the PCM's temperature, heat is transmitted from the PCM to the surrounding, resulting in a warming effect, and the PCM returns to its liquid state.

In this report, a simulation study of the PCM in the PVT system will be simulated using computational fluid dynamics, analyzed, and compared with existing PVT/PCM system of different properties of PCM. A simulation study on the effect of thickness of PCM to the electrical and thermal efficiency of the system will also be presented in this report.

1.2 PROBLEM STATEMENT

Water, air, or other working fluids are used to remove heat in PVT systems. Solar energy, on the other hand, changes significantly during the day, making it impractical to use a PVT device to generate thermal energy. Indeed, solar radiation is lowest in the evening when demand for heat is greatest. In these instances, latent thermal energy storage technologies such as phase change material (PCM) can be employed to store and release solar energy absorbed by photovoltaic (PV) devices. Combining a PCM with a PVT system not only maximizes solar energy use, but also enhances the energy efficiency of the system. The primary disadvantage of today's PCMs is their low thermal conductivity. Recent years have seen an increase in research aimed at resolving the problem. Increasing thermal conductivity increases heat storage and extraction rates during the melting and solidification processes

(Kazemian, Salari, Hakkaki-Fard, & Ma , 2019). Apart from thermal conductivity, there are several additional characteristics that might impact the performance of a PVT system including PCM, including the thickness of PCM, types of PCM, and the influence of melting temperature. All these distinct factors provide findings that may be utilized to enhance the performance of the PVT system, but they must be thoroughly examined, simulated, and suggested before they can be implemented in the PVT system.

1.3 OBJECTIVE

The objectives of this project are as follows:

1. To study the simulation of Photovoltaic Thermal (PVT) system using phase change material (PCM) using computational fluid dynamics
2. To propose the best PCM for the proposed PVT/PCM system in Malaysia.
3. To compare the PVT system's electrical and thermal efficiency of the PVT system incorporated with PCM of different thickness.

1.4 SCOPE OF PROJECT

The scopes of this project are as follows:

1. Only water-based PVT/PCM system are presented and studied in this report. Although there are many types of working fluid in the PVT/PCM system, however, the working fluid that is used in this report is water.
2. The CFD simulation of the PCM in PVT system will only be simulated and validated based on past research paper.
3. The CFD simulation will be done using 3D transient flow.

CHAPTER 2

LITERATURE REVIEW

2.1 INTRODUCTION

This chapter will cover the literature review that will be used in this project. The literature will contain information relating to the PVT systems incorporating with and without PCM, the comparison of PCM between previous research studies, and the existing design of PCM and its simulation works.

2.2 OVERVIEW OF PVT/PCM SYSTEM

A photovoltaic thermal system (PVT) is a kind of solar energy system that generates both electrical and thermal energy. When a photovoltaic panel is exposed to solar radiation, the solar irradiation's effect is converted to different forms of energy. The solar panel converts a portion of the energy it absorbs to electricity, while the remainder is absorbed by the cooling fluid that travels through the solar panel. Figure 2.1 depicts a schematic representation of the PVT system. Photovoltaic panels, batteries, pumps, and heat exchangers comprise the PVT framework. When solar irradiation strikes a photovoltaic panel, only a small proportion (7–20 percent) of it is converted to electrical energy. The remaining irradiation is converted to heat energy, lowering the solar module's efficiency, and shortening the panel's life. Often, either air or water is used to cool the solar modules.

The cooling fluid absorbs heat from the solar module by flowing through the back side of the module. The battery generates electrical energy and stores it for later use.

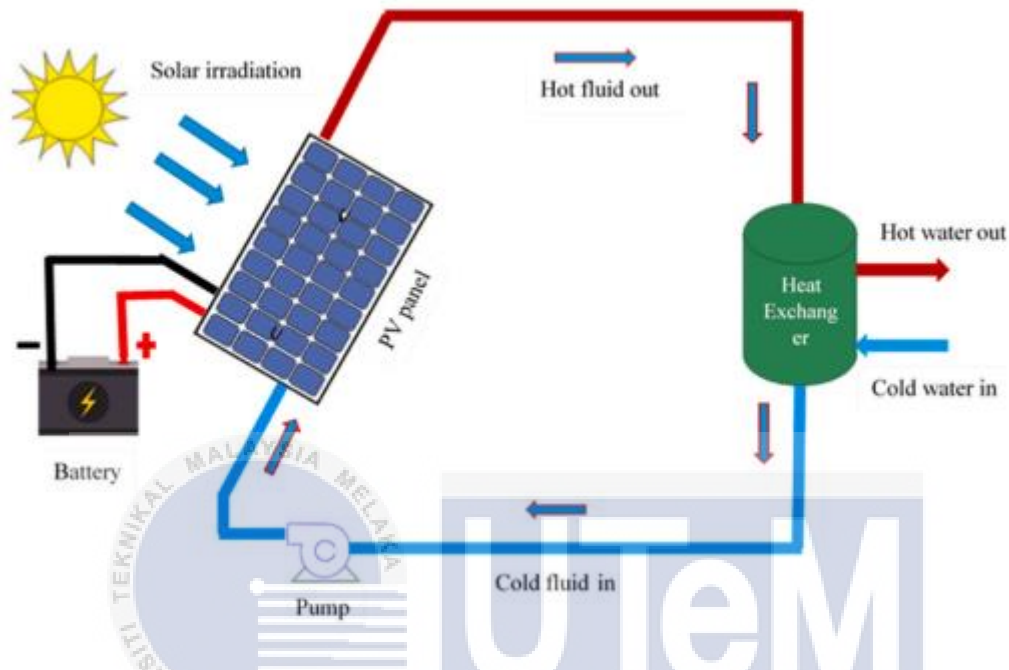


Figure 2.1 - schematic diagram of PVT system (Reji Kumar, Samykano, Pandey, Kadirgama, & Tyagi, 2020).

Solar thermal energy is capable of being stored in a variety of ways. Thermal energy storage is a method of using stored heat energy rather than dissipating it into the environment. Physical and chemical energy storage are both important means of storing energy. Each kind of thermal energy storage technology has a unique set of benefits and drawbacks. The heat transfer system conserves energy by using the physical approach of thermal energy storage, and the capacity of the material to store energy is determined by its thermophysical parameters. Energy is stored as internal energy in the form of latent and sensible heat in physical storage. Heat energy may be stored or released by raising or reducing the temperature of a medium during a sensible heating or cooling operation. Latent heat (LH) is the energy retained or released during the transformation of a material from

solid to liquid to solid and vice versa. (Tyagi, Reji Kumar, Samykano, Pandey, Kadirgama, and Kadirgama, 2020).

Thermal energy storage (TES) and latent heat storage materials are examples of PCMs. When a substance transitions from solid to liquid at constant temperature, heat may be kept inside the material or released when the material changes phase from liquid to solid. Per unit volume, PCMs can store 5–14 times the amount of heat as sensible heat (Reji Kumar, Samykano, Pandey, Kadirgama, & Tyagi, 2020).

2.3 PHASE CHANGE MATERIAL

A phase change material (PCM) is introduced here as a latent heat storage medium. It is also referred to as a substance that stores latent heat. When heated, cooled, or phase transitioned, it has the ability to store and release thermal energy.

Latent heat storage materials initially function similarly to sensible heat storage materials, since they absorb heat in the solid state as the temperature increases. When materials reach their melting point, however, they absorb heat at a constant rate equal to their melting point. After completely converting to the liquid state, the materials retain their ability to absorb heat in the liquid form. Thus, latent heat storage is more effective at storing heat per unit volume than sensible heat storage.

PCMs are employed in a variety of areas and serve as a thermal energy storage medium. Numerous researches have established that PCM enhances the performance of a wide number of applications. In PVT/PCM system, (Huang, Eames, & Norton, 2004) discovered that a PCM with an appropriate phase change transition temperature might help keep the PV cells cool due to the PCM's ability to store solar energy for an extended period of time. Due

to PCM's consistent heat storage capacity at constant temperature, it is advantageous to include a heat sink into the system for temperature management and performance improvement of PV/T (Waqas Adeel & Ji, 2017).

2.3.1 CLASSIFICATION OF PHASE CHANGE MATERIAL

There are various forms of PCM found across the globe, and they are normally classified according to the physical state of the material before to and during the phase transition process. PCMs are classified as solid-liquid, liquid-gas, or solid-gas.

Among the several types of PCMs, solid-liquid PCMs are the ones that are most commonly used in a wide array of technological applications. When compared to other types of PCMs, they benefit from a low volume change and a high latent heat capacity during the phase transition process. While phase transitions involving gases may yield enormous quantities of thermal energy, confining a large quantity of gas requires the use of a pressure vessel, which is costly and potentially dangerous. (Lin, Jia, Alva, & Fang, 2017).

Furthermore, there is another approach to classify PCMs based on their chemical composition. The categorization of phase change materials is depicted in the figure. They are classed as organic PCMs, inorganic PCMs, or eutectic PCMs.

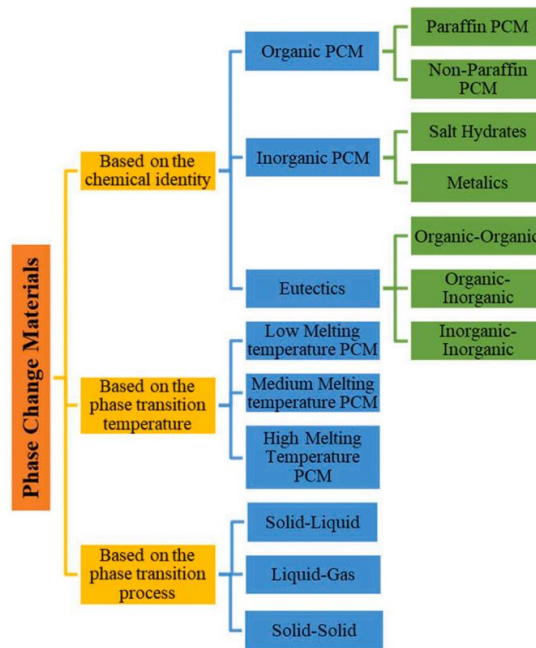


Figure 2.1- classification of PCMs (Reji Kumar, Samykano, Pandey , Kadirgama, & Tyagi, 2020).

Organic PCMs are further classed as paraffin and nonparaffin type, and they have the benefits of being nontoxic, noncorrosive, chemically stable, consistent melting, and have almost no supercooling. The disadvantage of organic PCMs are flammable and have a low thermal conductivity.

Moreover, when compared to organic PCMs, inorganic PCMs such as salt hydrates or metallics have the benefits of being less expensive, non-flammable, and having a high latent heat. However, there are a number of disadvantages, including a substantial volume change during the phase change process, limited temperature stability, and corrosive nature.

Eutectic PCMs, are PCMs that include two or more soluble compounds. They are often superior to organic and inorganic PCMs due to their high heat conductivity, lack of material separation during solidification, and simultaneous melting. However, eutectic PCMs is too expensive.

2.3.2 SELECTION CRITERIA FOR PHASE CHANGE MATERIAL

The selection of PCM for latent heat storage is mostly determined by the intended application, as each material has unique material characteristics. However, the most critical parameter to consider when selecting the appropriate PCM for latent heat storage is the material's thermal characteristics.

Firstly, it is necessary to know the phase change temperature of the substance. The operating temperature of the system for heating and cooling should match the phase change temperature of the PCM (Wang, et al., 2015).

Furthermore, the PCM's latent heat value and specific heat capacity should be high in both the liquid and solid forms to store more energy, since the PCM's purpose is to act as a thermal energy storage device and store heat energy. As more heat energy is conserved, thermal energy storage becomes more efficient.

Thermal conductivity of PCM is also a key consideration when selecting a material. Because thermal conductivity is crucial in charging and discharging process of thermal energy storage, a material with a high thermal conductivity is desired because it results in increased thermal energy storage performance.

Apart Apart from the thermal characteristics mentioned above, other factors such as physical, chemical, and kinetic qualities, as well as economic and market availability, should be addressed before choosing a material (Ibrahim, Al-Sulaiman, Rahman, Yilbas, & Sahin, 2017). The advantages of PCMs for latent heat storage are summarised in Table 2.1.

Table 2.1 - Desired properties of PCM.

Thermal Properties	<ul style="list-style-type: none"> - High thermal conductivity - High specific heat - Suitable melting temperature - High latent heat
Physical properties	<ul style="list-style-type: none"> - Low volume change - High density
Chemical Properties	<ul style="list-style-type: none"> - Non-flammable - Non-toxic - Non-corrosive - Long-term chemical stability
Kinetic Properties	<ul style="list-style-type: none"> - Rapid crystallization - Little to no supercooling
Economics	<ul style="list-style-type: none"> - Cost effective - Abundant - Availability in the market

2.4 EFFECT OF THICKNESS OF PCM IN PVT/PCM SYSTEM

According to a study made by (Su, Jia, Lin, & Fang , 2017), the thickness of the PCM layer is important in determining the energy output of the PVT collector. A PCM layer with a thickness higher than the optimum thickness of the PCM layer made in the study with relation to melting point, the thermal energy output of the system for 40 and 50 °C melting point starting to decrease after a certain point of thickness while the thermal energy output

for 30 °C melting point is gradually decreasing while for 60 °C melting point, the thermal energy output for the system remains unchanged.

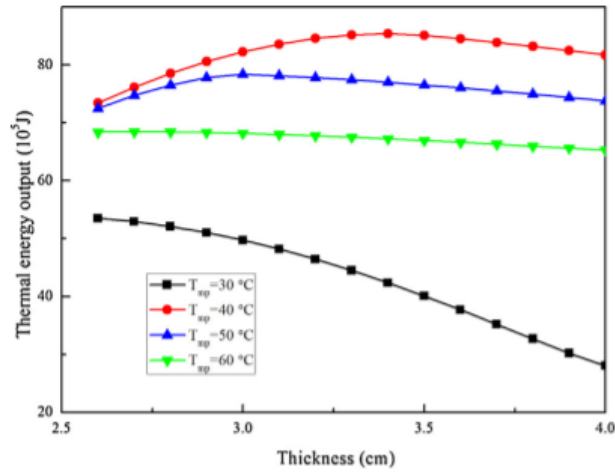


Figure 2.2 - thermal energy output with varying PCM thickness (Su, Jia, Lin, & Fang , 2017).

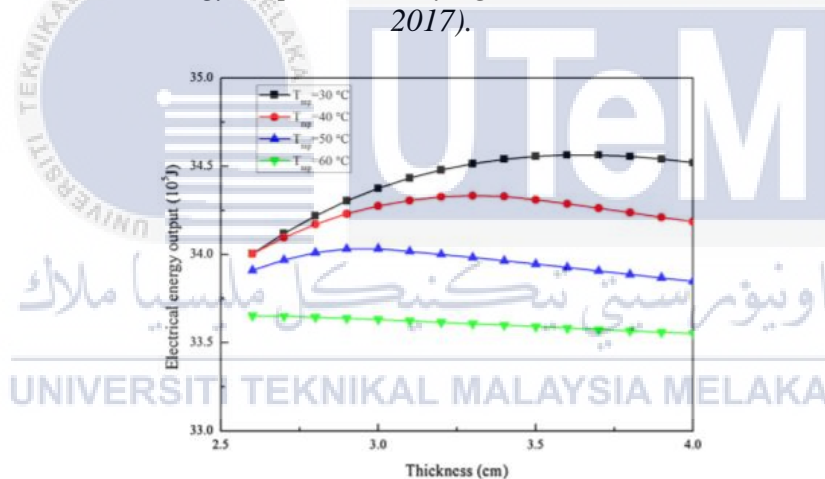


Figure 2.3 - electrical energy output for varying PCM thickness (Su, Jia, Lin, & Fang , 2017).

From Figure 2.3, the electrical energy output of the system shows that the PCM with the lowest melting point has the higher electrical energy output. This is because, the thicker the PCM layer, the greater its thermal capacity, but the lower the heat transfer coefficient between the PV module and the PCM layer (Su, Jia, Lin, & Fang , 2017). However, the thickness of the PCM layer for PVT system must be selected properly with balanced thermal and electrical energy output so that an optimum performance of the system can be achieved.

In this case, (Su, Jia, Lin, & Fang , 2017) has concluded that a 3.4 cm-thick PCM layer with 40°C melting point gives the optimum efficiency compared to other PCM layer thickness with varying melting point.

According to (Malvi, Dixon-Hardy, & Crook, 2011), the thickness of PCM from 0 to 3 cm can increase the electrical energy output by 6.5%. Increasing the thickness of PCM layer beyond 3 cm will give no value to the system as the electrical energy output of the PCM corresponds to the deepest point that the melting front can reach. The deeper the thickness of the PCM layer from the point where the heat can reach, the harder it is for the PCM to absorb heat from the outside surface, hence making the remaining depth of the PCM to be almost useless to the system.

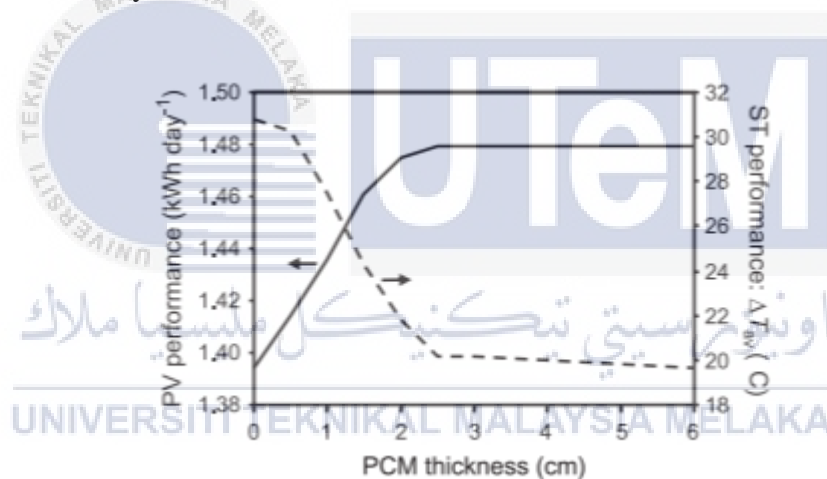


Figure 2.4 - effect of PCM thickness to the performance of PVT (Malvi, Dixon-Hardy, & Crook, 2011).

An experimental and simulation study conducted by (Indartono, Prakoso, Suwono, Zaini, & Fernaldi, 2015) to determine whether the PCM thickness can decrease the temperature of the PV module. From their observation, the thicker the PCM layer mounted on the PV module, the greater the temperature drop experienced by the module.

An experimental and numerical investigation made by (Yuan, et al., 2018), they have investigated the influence of PCM thickness in PVT system at day and night-time in China.

They have concluded that the temperature of the PCM can decrease as the thickness of the PCM increase. They have also stated that using thicker PCM can enhance their antifreeze function at night-time and also decrease the final water temperature at daytime.

2.5 EFFECT OF PROPERTIES OF PCM IN PVT/PCM SYSTEM

In this part, the effect of the properties of the PCM will be discussed. The effect of the type of PCM used, the effect of melting temperature, and the effect of thermal conductivity used in numerical and experimental investigation will be discussed.

2.5.1 THE EFFECT OF MELTING TEMPERATURE OF THE PCM

The melting temperature of the PCM is the most common and popular parameter that are always being studied in PVT/PCM system. This is because, the melting temperature of the PCM determines the melting and solidification time of the PCM and a suitable melting temperature has to be analysed for a good thermal performance of the PCM.

(Kazemian, Salari, Hakkaki-Fard, & Ma , 2019) have studied the effect of operating conditions on the melting performance of the PCM by simulating different solar radiation. They have noticed that higher solar radiation caused the PCM to melt more due to increasing heat absorption from the PCM. This concludes that with a suitable melting point, too high or too low solar melting point can cause ineffectiveness to the PCM as it needs more heat to melt itself.

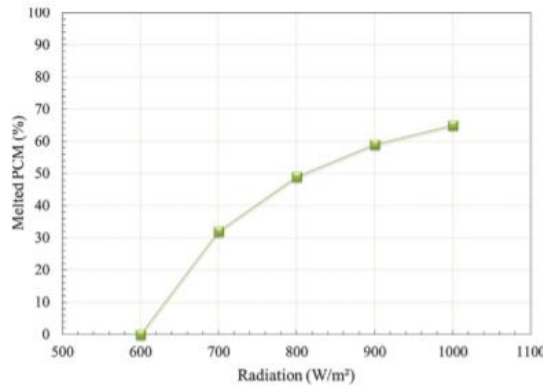


Figure 2.5 - effect of solar radiation to the melted PCM (Kazemian, Salari, Hakkaki-Fard, & Ma , 2019).

(Su, Jia, Lin, & Fang , 2017) and (Yuan, et al., 2018) both have studied the impact of thermal and electrical performance of the PVT/PCM system due to different melting point. (Su, Jia, Lin, & Fang , 2017) have studied the simulation effect of different types of different PCM with different melting point and investigated their electrical and thermal efficiency of the system. They have found that different melting points of the PCM contributed a lot to the PV cell temperature. A higher cell temperature is linked to the PCM with higher melting point and the highest cell temperature of the PV is when no PCM is integrated into the system. They have also found that the heat energy stored by the PCM can be extricated easily compared to others. The electrical efficiency of the PCM with higher melting point is lower compared to the PCM with lower melting point.

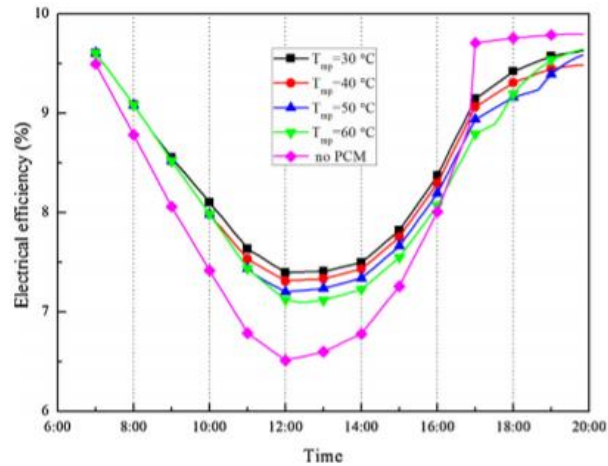


Figure 2.6 - electrical efficiency for different melting point (Su, Jia, Lin, & Fang , 2017).

Besides, (Su, Jia, Lin, & Fang , 2017) have also studied the thermal efficiency for the system. In their study, the increase in difference in temperature leads to an increase in heat flow rate and the highest melting point of the PCM releases heat quickly as their thermal conductivity increases.

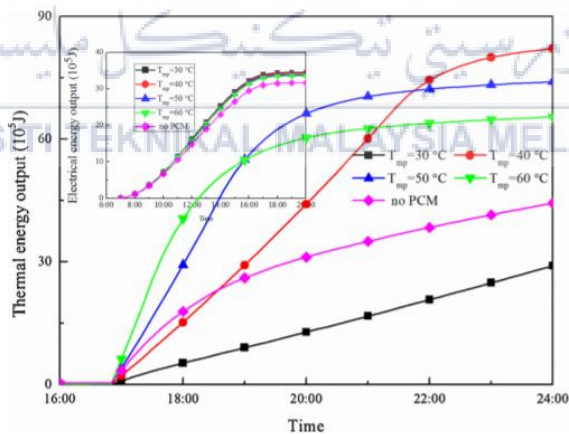


Figure 2.7 - thermal energy output for varying melting point (Su, Jia, Lin, & Fang , 2017).

On the other hand, a study made by (Yuan, et al., 2018) have also emphasize the effect of melting temperature of the PCM in their study. In their study, they have mentioned that the melting temperature of the PCM has to be higher than the ambient temperature in order

to decrease the temperature of the PV module. They have also mentioned the importance of the melting temperature to avoid the freezing of water in the solar collector system. By adjusting the melting temperature of the PCM to an optimum level, the melting time of the PCM will be increased and the freezing of the system can be dodged.

2.5.3 EFFECT OF THERMAL CONDUCTIVITY TO THE PVT/PCM SYSTEM

The effect of thermal conductivity to the thermal and electrical performance of the PVT/PCM system is also an important factor in the system. (Kazemian, Salari, Hakkaki-Fard, & Ma , 2019) have investigated that the thermal conductivity can affect other parameter like the melting of the PCM, coolant outlet temperature, surface temperature, electrical and thermal performance of the system.

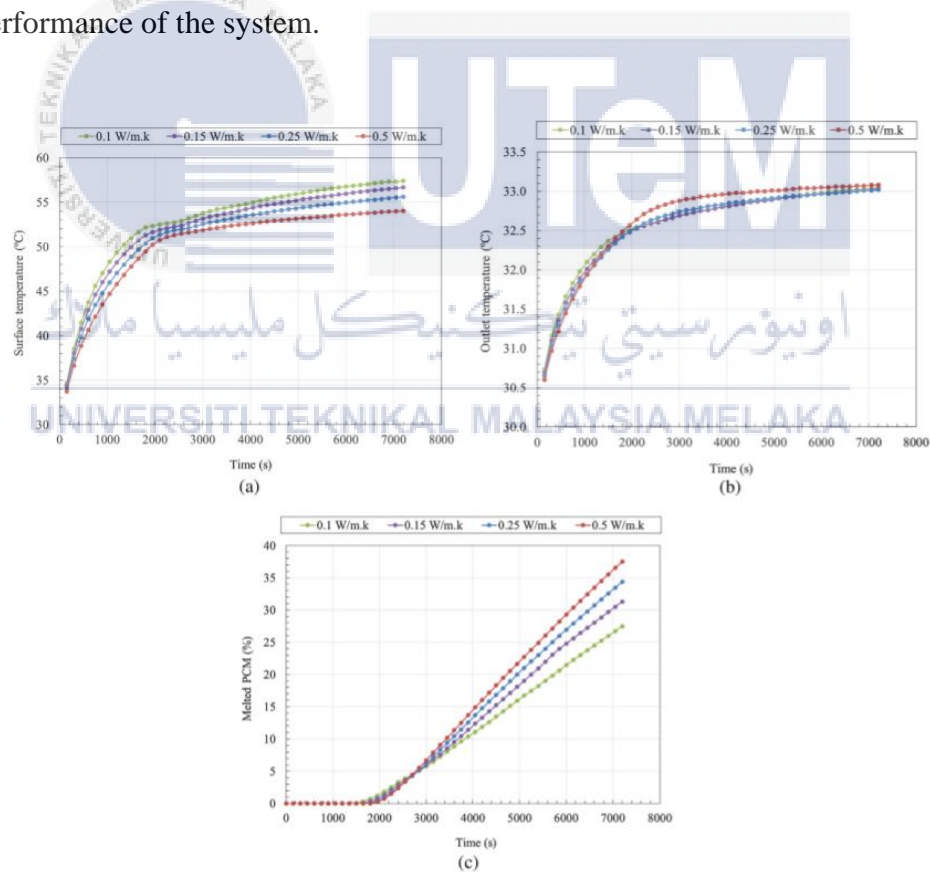


Figure 2.8 - effect of thermal conductivity to different parameter to PCM (Kazemian, Salari, Hakkaki-Fard, & Ma , 2019).

Based on Figure 2.17, (Kazemian, Salari, Hakkaki-Fard, & Ma , 2019) have concluded that increasing thermal conductivity can reduce surface temperature of the system and as more heat can be conducted into the PCM. The outlet temperature of the system increases as thermal conductivity increases because the energy absorption rate of the PCM increases. The percentage of PCM that is melted through the simulation also studied and as the percentage of melted PCM also increases as thermal conductivity increases. Finally, the thermal and electrical efficiency of the system are also enhanced significantly with the increment of thermal conductivity.

Finally, (Mousavi, Kasaeian, Behshad Shafii, & Hossein Jahangir, 2018) has incorporated metal foam into the PVT/PCM system to enhance the thermal conductivity of the PCM and improve overall temperature distribution. To compare, (Kazemian, Salari, Hakkaki-Fard, & Ma , 2019) approach involves less cost because it does not involve a design changes to the PCM system while (Mousavi, Kasaeian, Behshad Shafii, & Hossein Jahangir, 2018) approach to enhance the thermal conductivity of the system is more efficient and has stable temperature distribution due to the integration of the metal foam.

2.5.3.1 DISADVANTAGEOUS OF LOW THERMAL CONDUCTIVITY OF PCM

Although pure PCMs have a high latent heat that allows them to store thermal energy, their cooling capacity and storage efficiency are restricted by their poor thermal conductivity ($1 \text{ W}/(\text{m K})$) when compared to metals ($100 \text{ W}/(\text{m K})$) (I. & A., 2019), (A. , V.V., C.R., & D., 2009). PCMs with high latent heat and high heat conductivity are required to obtain high energy density and cooling capacity. The melting temperature, latent heat, and thermal conductivity of the PCM are significant thermophysical properties for thermal storage. The temperature range for which the PCM thermal storage is effective is determined by the melting temperature. The latent heat represents the PCM's energy density throughout storage

and release cycles. The charge or discharge rate of thermal energy, also known as cooling power, is governed by thermal conductivity (Yang, King, & Miljkovic, 2021). Thus, having low thermal conductivity can affect the charging and discharging rate of the PCM and also have a slower heat transfer process, compared to materials that has high thermal conductivity.

Metal alloy PCMs have a greater melting temperature, volumetric latent heat, and thermal conductivity than organic PCMs. Metal alloys become more attractive for high temperature and high heat flux applications as a result of this. However, Organics and salts with greater specific latent heat are useful for applications needing high specific power density (Yang, King, & Miljkovic, 2021). According to the second law of thermodynamics, heat will always be transferred from a high temperature zone to a low temperature region anytime there is a temperature difference. As a result, heat transfer is a fairly prevalent phenomena in both nature and engineering technology. Thermal conduction, thermal convection, and thermal radiation are the three basic ways of heat transfer. The thermal conduction mode, as opposed to the thermal convection and radiation modes, is the most frequent and effective technique of performing the thermal transportation process, and hence the most common and effective heat transfer mode in PCMs (Yuan, et al., 2019).

Table 2.2 - Example of types and properties of PCM used in previous studies.

Referenc e	PCM	Melting temperatu re (°C)	Heat capaci ty (J/kg. K)	Thermal conductivi ty (W/m.K)	Latent heat (J/kg)	Enthal py of fusion (kJ/kg)	Densit y (kg/m³)
(Kazemia n, Salari, Hakkaki- Fard, &	Not specified	55	2300	0.25	Not specifi ed	170	800

(Ma, 2019)							
(Mousavi, Kasaeian, Behshad Shafii, & Hossein Jahangir, 2018)	Paraffin C18	29	2520	Not specified	Not specified	244	760 (l) 900(s)
	Paraffin C22	46	2950 (l) 2510 (s)	Not specified	Not specified	226	760 (l) 818 (s)
	Palmitic acid/Capric acid	17.7 – 122.8	1650	Not specified	Not specified	190	883
	Sodium phosphate salt	37	1690(l) 1940 (s)	Not specified	Not specified	280	1522
	Paraffin C15	14	2520	Not specified	Not specified	205	760 (l) 900 (s)
(Badiei, Eslami, & Jafarpur, 2019)	PCM-1	35.4 – 36.4	2400 (l) 1926 (s)	0.146 (l) 0.423 (s)	2.48×10^5	Not specified	769 (l) 910 (s)
	PCM-2	42 – 44	2411 (l) 2052 (s)	0.15 (l) 0.4 (s)	1.68×10^5	Not specified	760 (l) 844 (s)
	PCM-3	50 – 52	1863 (l) 1650 (s)	0.15 (l) 0.4 (s)	2.00×10^5	Not specified	767 (l) 848 (s)
	PCM-4	60 - 62	2384 (l) 1850 (s)	0.15 (l) 0.4 (s)	2.09×10^5	Not specified	778 (l) 861 (s)
(Su, Jia, Lin, &)	Not specified	22.8	2100 (l)	0.15 (l) 0.24 (s)	2.10×10^5	Not specified	780 (l) 860 (s)

Fang , 2017)			2900 (s)				
(Yuan, et al., 2018)	Not specified	15.15	1500	0.2	1.82 x 10 ⁵	Not specifie d	673.47

2.6 PREVIOUS STUDIES ABOUT PVT/PCM SYSTEM

In this part, a general comparison about past studies about PVT/PCM system. The comparison will consist of the type of investigation used in the studies, major findings, type of analysis used in their studies, and the parameters considered in the study

(Kazemian, Salari, Hakkaki-Fard, & Ma , 2019) have investigated the effect of important parameters such as the enthalpy of fusion, solar irradiation, melting temperature, mass flow rate, and thermal conductivity to the thermal and electrical performance of the PVT/PCM system and has found that the increase of thermal conductivity can increase the thermal conductivity of the system, which was also agreed by the simulation study made by (Mousavi, Kasaeian, Behshad Shafii, & Hossein Jahangir, 2018) where they have added metal foam as a porous media integrated with the PCM for the enhancement of the thermal conductivity of the PVT/PCM system. (Mousavi, Kasaeian, Behshad Shafii, & Hossein Jahangir, 2018) have also included the effect of mass flow rate in their study and have concluded that by setting the mass flow rate of 0.02 kg/s with Paraffin C22 as heat storage material, the system has the best thermal performance compared to others. A simulation study made by (Badiei, Eslami, & Jafarpur, 2019) for the behaviour of PCM in winter and summer condition in Iran, they have proven that the effectiveness of the PCM can be enhanced by using fins and with a higher melting temperature while a lower melting point is more suitable for enhancing the performance of the PCM when fins are not added and this

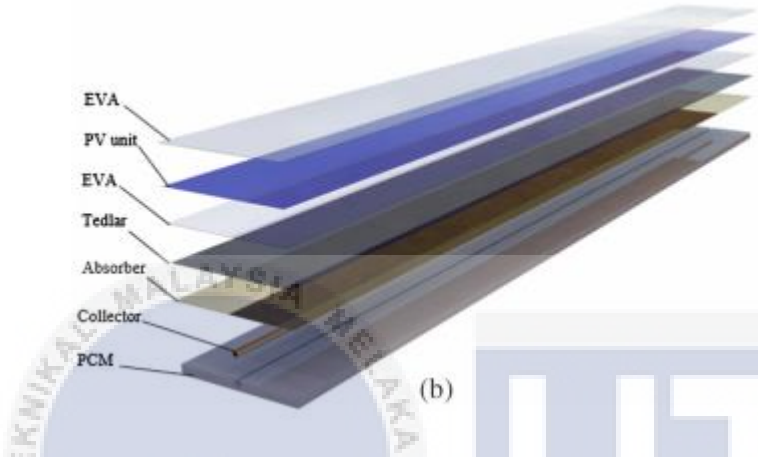

statement has been supported by the comparative analysis made by (Su, Jia, Lin, & Fang , 2017). Finally, (Yuan, et al., 2018) and (Su, Jia, Lin, & Fang , 2017) have also studied the effect of thickness of the PCM and have obtained that the optimum thickness of the PCM that is required for maximum performance of the system is around 3 cm. they have also agreed that increasing the thickness of the PCM can enhance the performance of the PVT/PCM system



2.7 MODEL COMPARISON

Table 2.3 - model comparison of previous studies.

No.	Reference	Model	Components	Dimension (mm)
1.	(Kazemian, Salari, Hakkaki-Fard, & Ma , 2019)		PCM	1640 x 200 x 15
			EVA	1640 x 200 x 0.5
			PV unit	1640 x 200 x 0.3
			Tedlar	1640 x 200 x 0.1
			Copper absorber plate	1640 x 200 x 0.4
			Outer diameter of collector pipes	10
			Remarks:	<ul style="list-style-type: none"> - All dimensions are in sequence of (L x W x H).

		 <p data-bbox="616 667 1355 694"><i>Figure 2.9 - schematic diagram of (a) PVT, and (b) PVT/PCM.</i></p>		<p data-bbox="1881 199 2038 518">The dimension of both (a) and (b) are all the same except for PCM.</p>								
2.	(Mousavi, Kasaeian, Behshad Shafii, & Hossein Jahangir, 2018)		<table border="1"> <tr> <td data-bbox="1500 794 1774 877">PV panel</td> <td data-bbox="1780 794 2042 877">1600 x 1000</td> </tr> <tr> <td data-bbox="1500 877 1774 981">Absorber plate</td> <td data-bbox="1780 877 2042 981">1600 x 1000 x 2</td> </tr> <tr> <td data-bbox="1500 981 1774 1125">Sheet-and-tube exchanger</td> <td data-bbox="1780 981 2042 1125">Outer diameter: 10 Tube thickness: 1</td> </tr> <tr> <td data-bbox="1500 1125 1774 1228">Container</td> <td data-bbox="1780 1125 2042 1228">1600 x 1000</td> </tr> </table>	PV panel	1600 x 1000	Absorber plate	1600 x 1000 x 2	Sheet-and-tube exchanger	Outer diameter: 10 Tube thickness: 1	Container	1600 x 1000	
PV panel	1600 x 1000											
Absorber plate	1600 x 1000 x 2											
Sheet-and-tube exchanger	Outer diameter: 10 Tube thickness: 1											
Container	1600 x 1000											

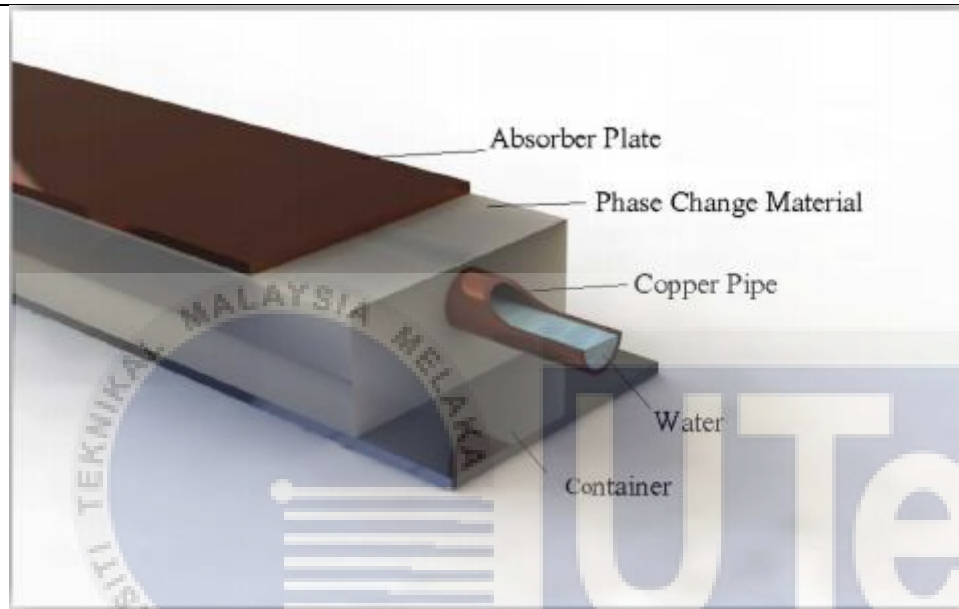


Figure 2.10 - schematic diagram of the simulation model.

Remarks:
 All dimensions are in sequence of (L x W x H).
 The dimension of both (a) and (b) are all the same except for PCM.

4.	(Su, Jia, Lin, & Fang, 2017)	PV module	Length: 1800 Width: 1000
		Pipe	Diameter: 25.4 Thickness: 0.8
		PCM	Thickness: 50

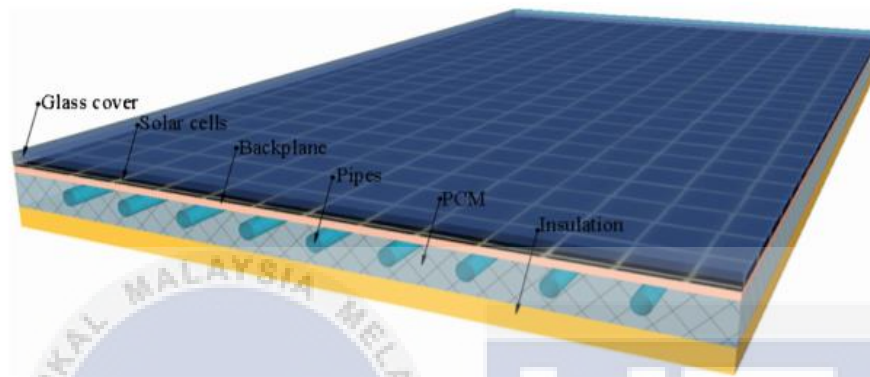


Figure 2.11 - schematic diagram of PVT collector with PCM.

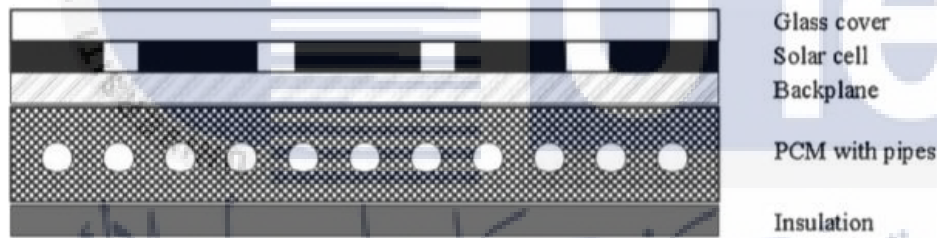
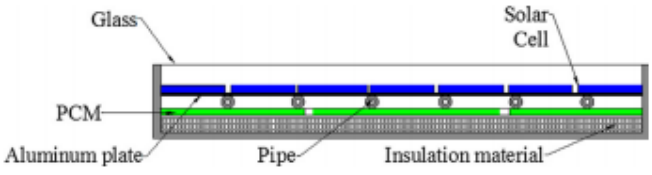


Figure 2.12- sectional view of the PVT collector with PCM.

Glass cover	Thickness: 5
Solar cell	Thickness: 0.3
Backplane	Thickness: 0.1
Insulation	Thickness: 50
Pipe	Length: 1214 Thickness: 10
PCM	Thickness: 50

5. (Yuan, et al., 2018)

	 <p data-bbox="622 427 1348 459"><i>Figure 2.13 - schematic diagram of PVT collector with PCM.</i></p>	PV module	Height: 860 Length: 1214 Width: 22
--	--	-----------	--

The incorporation of copper pipes as water collector is quite common in PVT/PCM system. This can be seen from Table 2.3 as all PVT/PCM system mentioned in the table have used copper pipe as their main water collector. (Mousavi, Kasaeian, Behshad Shafii, & Hossein Jahangir, 2018) have integrated metal foam to enhance the thermal conductivity of the PCM. Finally, (Kazemian, Salari, Hakkaki-Fard, & Ma, 2019), (Su, Jia, Lin, & Fang, 2017), and (Yuan, et al., 2018) almost have the same model configurations but with different size and dimension.

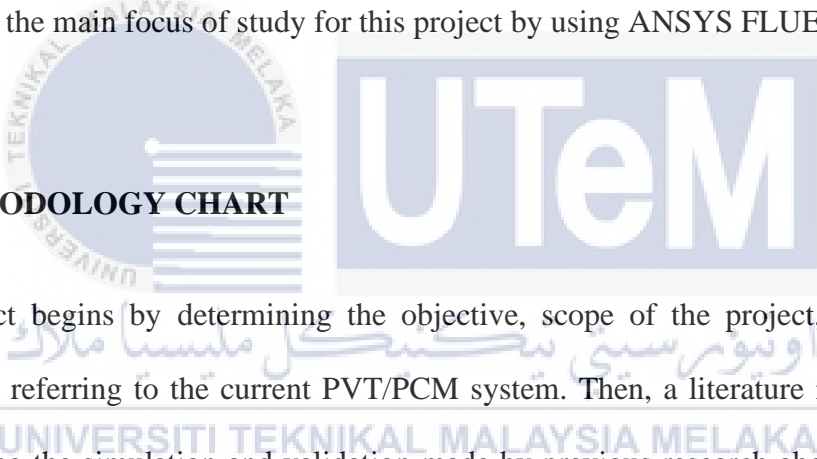
CHAPTER 3

METHODOLOGY

3.1 INTRODUCTION

The details of methodology used in this project for PVT system incorporated with PCM will be explained in this chapter. The actions that will be carried out to achieve the objectives of this project will also be explained in this chapter. Next, the validation process will also be presented and explained in detail. The simulation study of the PVT system incorporated with PCM will be the main focus of study for this project by using ANSYS FLUENT software.

3.2 METHODOLOGY CHART



The project begins by determining the objective, scope of the project, and problem statement by referring to the current PVT/PCM system. Then, a literature review will be made studying the simulation and validation made by previous research about the system. After a thorough research has been made from the research papers, a model will be taken and simulated exactly as the reference paper by using ANSYS FLUENT software to make sure that the same outcome can be produced from the reference paper for future work of this project. Next, the simulation and validation made that has the least error will be chosen for future improvement of the PVT/PCM system. The model will be altered based on the proposed solution for the improvement of this project. The new model will be simulated and analysed.

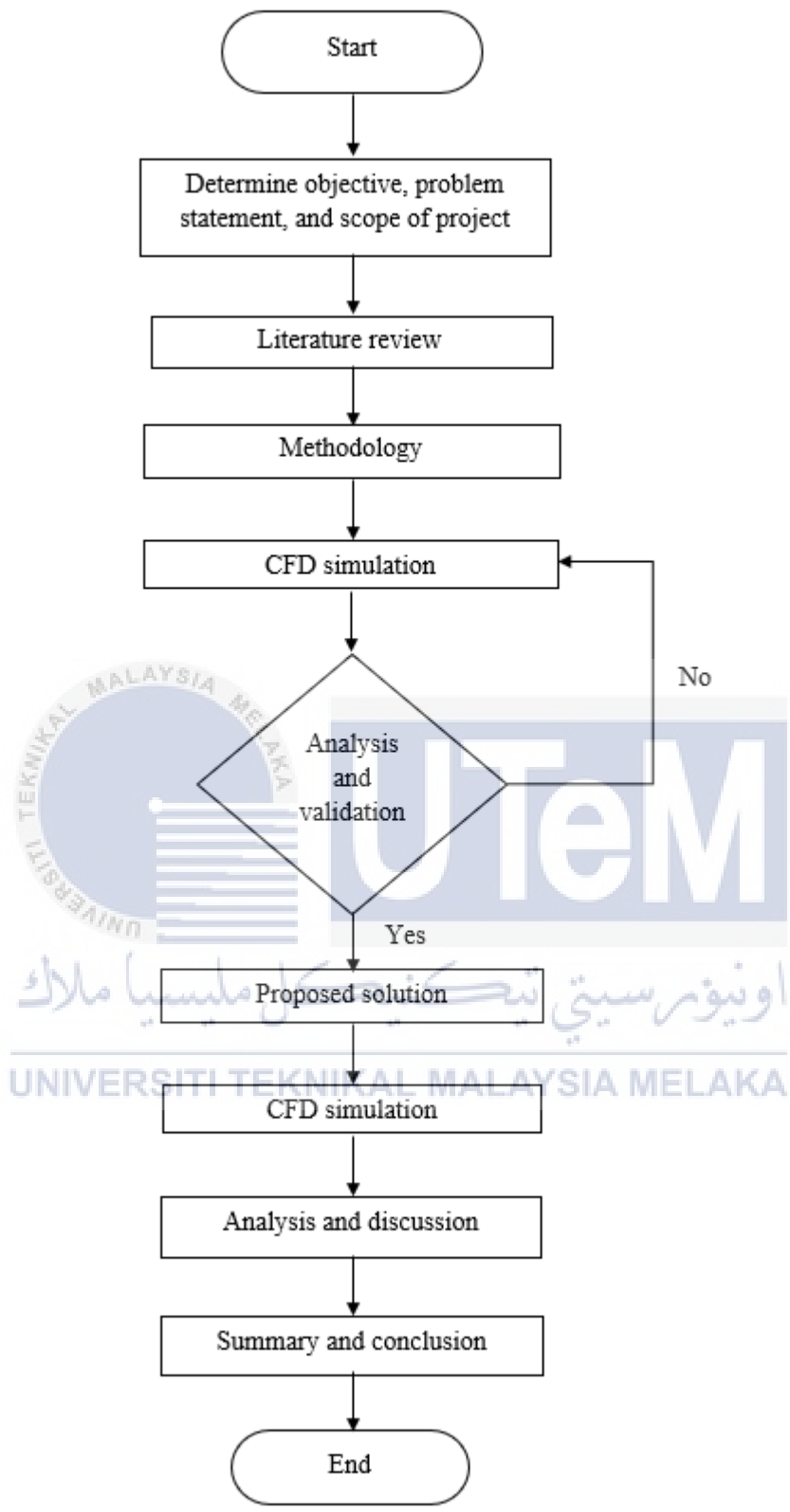


Figure 3.1 - flow chart of methodology of the project.

3.3 SIMULATION PROCEDURE

The simulation procedure will be presented step by step in this part of the study.

3.3.1 SIMULATION SETUP

The simulation set up for this project are as seen on Figure 3.2 below. The geometry of the model used in this study is based on the numerical analysis of (Kazemian, Salari, Hakkaki-Fard, & Ma , 2019). The reference model was selected because the information of the simulation of the model stated in the paper is adequate compared to other reference papers. The model is replicated, simulated, and validated before a solution to enhance the performance of the model can be proposed. The model used in the study is drawn by using Solidworks software. The components that are involved in the simulation consists of a PV unit surrounded by EVA layer on top and below of the PV surface, tedlar, a sheet and tube copper collector, and a PCM layer. The comparison of the model that is replicated from the paper can be seen in Figure 3.2 and Figure 3.3 while the dimensions of the parts of the model are presented in Table 3.1.

Table 3.1 - PVT/PCM system model dimension (Kazemian, Salari, Hakkaki-Fard, & Ma , 2019).

Components	Dimensions (m)
EVA	$1.64 \times 0.2 \times 0.0005$
PV	$1.64 \times 0.2 \times 0.0003$
Tedlar	$1.64 \times 0.2 \times 0.0001$
Copper absorber plate	$1.64 \times 0.2 \times 0.0004$
Collector pipe outer diameter	0.01
PCM	$1.64 \times 0.2 \times 0.015$

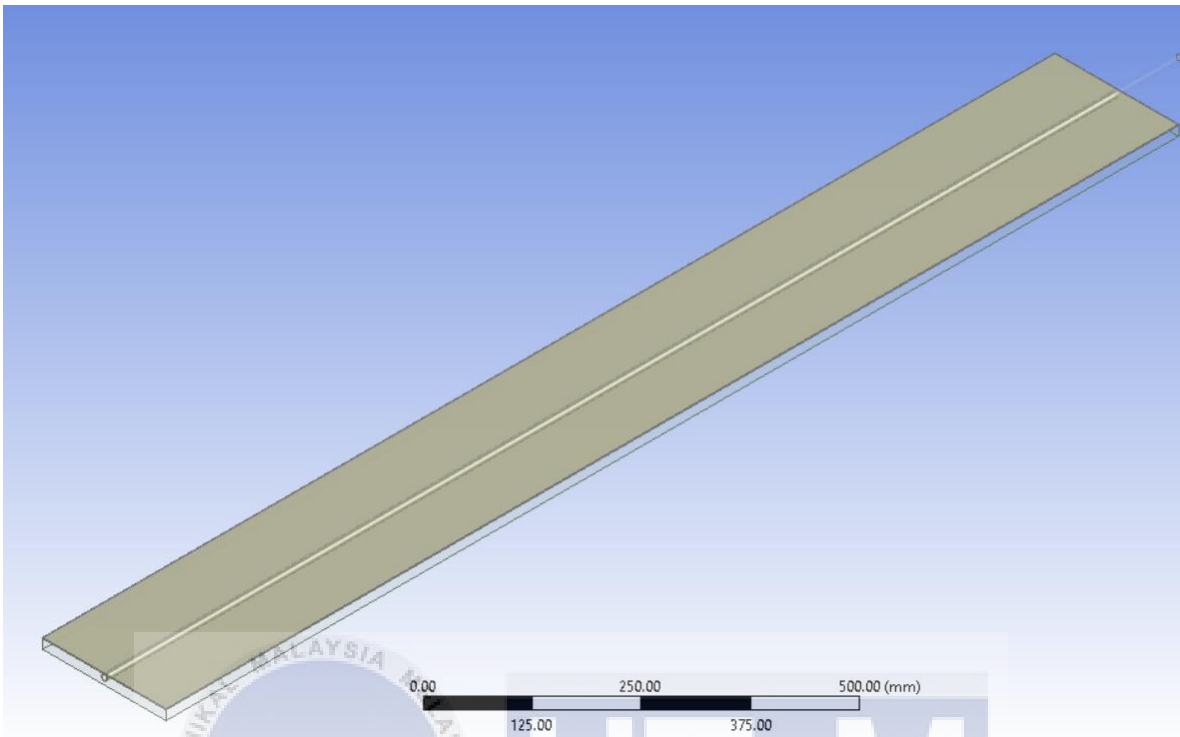


Figure 3.2 - isometric view of the model.

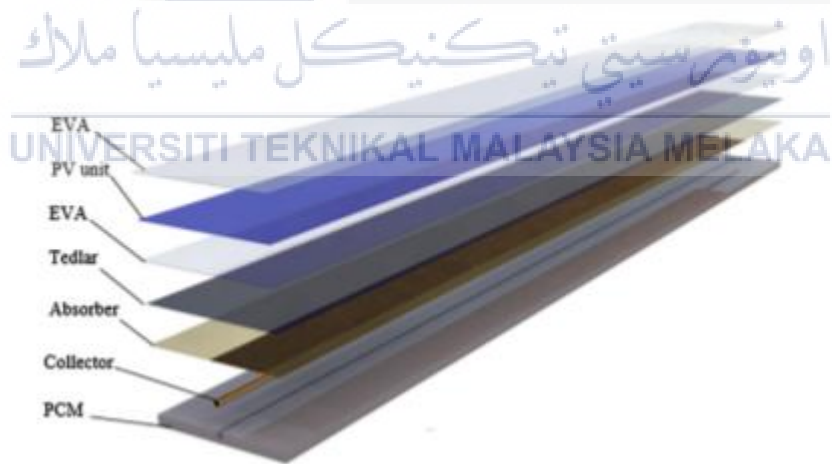


Figure 3.3 - schematic diagram of the reference model (Kazemian, Salari, Hakkaki-Fard, & Ma , 2019).

3.3.2 INITIAL AND BOUNDARY CONDITIONS

The boundary conditions for this simulation study are important in order to determine the right solution for the ANSYS FLUENT solver. The boundary conditions of this simulation will also be replicated from (Kazemian, Salari, Hakkaki-Fard, & Ma , 2019).

- The initial temperature for all parts of the system is 30 °C
- The initial mass flow rate for the working fluid is 30 kg/s and constant during the simulation
- The inlet of the model is mass-flow inlet and pressure outlet
- The walls in the boundary conditions are considered as “no slip” and “impermeable”
- PCM back walls and PV side walls are considered as adiabatic and no heat flux
- The absorbed solar radiation is equals to the PV cells heat generation rate
- The heat transfer by the glass surface to the surrounding is assumed to be both by convection and radiation
- Different surfaces of different parts of the model have the “interface” boundary conditions

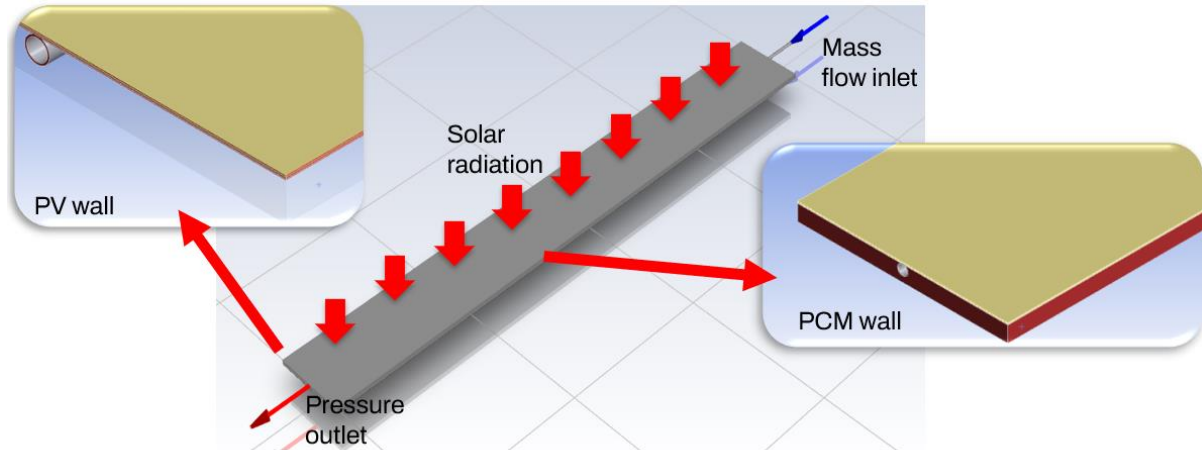


Figure 3.4 - boundary conditions of the present study presented in ANSYS Fluent software.

3.3.3 FLUID FLOW FEATURES AND SIMULATION ASSUMPTIONS

The simulation assumptions used by the model are based on the previous research on the PVT/PCM system.

- The mass flow rate of the working fluid in the copper collector tube is 30 kg/h and the flow is considered laminar.
- The fluid flow inside the collector tube is considered uniform, fully developed, and incompressible
- The thermophysical properties of the solid parts in the model are independent of temperature (Kazemian, Salari, Hakkaki-Fard, & Ma , 2019)
- The contact resistance between EVA, PV, Tedlar, and Sheet-and-tube collector can be neglected.
- The sky temperature in the system can be assumed as black body temperature
- The properties of the PCM are considered as constant in numerical simulation
- External agents such as dust and water on the surface of the PV can be neglected

- Incident solar radiation can be considered to be consistent and generates in the uppermost layer of PV unit, which is EVA
- The liquid phase of PCM is said to be three dimensional, incompressible, Newtonian, with an unsteady flow
- Homogenous and isotropic for both solid and liquid phases of PCM are considered
- The EVA layer has the transmissivity of 100%

3.3.4 GOVERNING EQUATIONS

The present work simulates a full 3D model of a PVT/PCM system under unstable conditions in order to examine the effect of utilising different kinds and thicknesses of PCM. Additionally, the bulk of solar irradiation used as input energy is absorbed by the photovoltaic unit, and a portion of it is lost to convection and radiation from the photovoltaic surface. The absorbed energy is transferred to several system components, including the working fluid and PCM. Using the PVT/PCM system as the control volume, the governing equations for the various components of the PVT/PCM system are listed below.

3.3.4.1 WORKING FLUID

The mass and momentum conservations for working fluid are denoted by the following equations:

$$\rho_f \left[\frac{\partial \vec{V}_f}{\partial t} + (\vec{V}_f \cdot \nabla) \vec{V}_f \right] = -\nabla P + \nabla \cdot (\mu_f \nabla \vec{V}_f) \quad (3.1)$$

where \vec{V} , P and μ are fluid velocity, pressure and viscosity and subscript “ f ” represents working fluid. Within the collector's fluid field, heat transmission occurs by a mix of conduction and convection. As a consequence, the following energy equation is given:

$$\rho C_p \frac{\partial T_f}{\partial t} + \rho_f C_{p,f} \vec{V}_f \cdot \nabla T_f = \nabla \cdot (k_f \nabla T_f) \quad (3.2)$$

3.3.4.2 SOLID COMPONENTS

Because the heat transfer process in the system's solid components is solely conduction, the energy equation for these components is as follows:

$$\rho C_{p,s} \frac{\partial T_s}{\partial t} = \nabla \cdot (k_s \nabla T_s) \quad (3.3)$$

Where “s” refers to solid components.

3.3.4.3 PHASE CHANGE MATERIAL

The present work employs an enthalpy-porosity approach to mimic the melting process in PCM. The melt interface is not explicitly recorded in this procedure. Indeed, each cell in the solution region utilises a liquid fraction (the proportion of cell volume that is liquid). An enthalpy balance is employed to determine the liquid fraction. The mushy zone (with a liquid percentage ranging from 0 to 1) is modelled in this model as a "pseudo" porous zone with a porosity ranging from 0 to 1.

$$\rho \left[\frac{\partial \vec{V}}{\partial t} + (\vec{V} \cdot \nabla) \vec{V} \right] = -\nabla P + \nabla \cdot (\mu \nabla \vec{V}) + S \quad (3.4)$$

$$S = \frac{(1-\beta)^2}{(\beta^3 + \phi)} A_{mush} (\vec{V} - \vec{V}_p) \quad (3.5)$$

where β is the liquid volume fraction, A_{mush} is mushy zone constant, which is equal to 100000, \vec{V}_p is the solid velocity as a result of the withdrawal of solidified material from the field, ϕ is a small quantity to avoid division by zero and equals 0.001. The energy equation is denoted by the following:

$$\frac{\partial}{\partial t} (\rho H) + \nabla \cdot (\rho \vec{V} H) = \nabla \cdot (k \nabla T) + S \quad (3.6)$$

where H , ρ , \vec{V} and S denote the enthalpy of the material, the density of the fluid, and the source term, respectively. The enthalpy of a substance is the total of its sensible and latent heat, and it may be computed as follows:

$$H = h + \Delta H \quad (3.7)$$

where h and denotes the sensible enthalpy and ΔH denotes the latent enthalpy. Sensible enthalpy is computed as follows:

$$h = h_{ref} + \int_{T_{ref}}^T C_p dT \quad (3.8)$$

where h_{ref} denotes the reference enthalpy at T_{ref} 's reference temperature. Additionally, the latent heat may be expressed as:

$$\Delta H = \beta L \quad (3.9)$$

where L is the material's latent heat, which can range from 0 (for a solid) to L (for a liquid), and β is the liquid fraction, which is defined as follows.:

$$\beta = \frac{T - T_{solidus}}{T_{liquidus} - T_{solidus}} \quad \text{if } T_{solidus} < T < T_{liquidus} \quad (3.10)$$

$$\beta = 0 \quad \text{if } T \leq T_{solidus} \quad (3.11)$$

$$\beta = 1 \quad \text{else } T \geq T_{liquidus} \quad (3.12)$$

3.3.5 NUMERICAL METHOD

The numerical methods and the simulation approach for this current study are presented in this subchapter.

- A CFD method using ANSYS FLUENT software are implemented in this study
- A pressure based approach is employed to the model to solve governing equations
-
- The fluid flow is considered laminar because the Reynolds number are below 2300
- SIMPLE method is used to provide the pressure-velocity coupling
- The second order upwind method are applied to discretize the convection terms
- The solutions are considered converged when the residuals are lower than 10^{-6} for momentum, 10^{-6} for continuity, and 10^{-8} for energy equations
- To mimic the solidification and melting of the PCM, the enthalpy-porosity approach is applied.
- The density, viscosity, and thermal conductivity of the PCM are considered constant
- A transient solver is used to solve the numerical equations
- The atmosphere temperature changes, and wind velocity are abandoned during the simulation
- The number of time step, time step size, and the maximum iterations per time step are 48, 150s, and 20, respectively.

3.3.6 MESHING

For meshing, there are a few methods that is used to provide more accurate results for the simulation in ANSYS Fluent. The sweep method has been used to mesh the faces of the volume of the model. All bodies of the model are chosen for this meshing method. A sweep method is important in this study to reduce the mesh cell counts and maintain high solver accuracy as well as speeding up the solving time. To make up a more accurate mesh results and quality, the inflation of mesh around the working fluid are applied and edge sizing along the edges of the model are also applied. A patch conforming method are also applied at the working fluid where a tetrahedral mesh is created. Edge sizing along the edges of different layers of the model and the regions around the solar collector are also applied to enhance the solver accuracy near the working fluid zones.

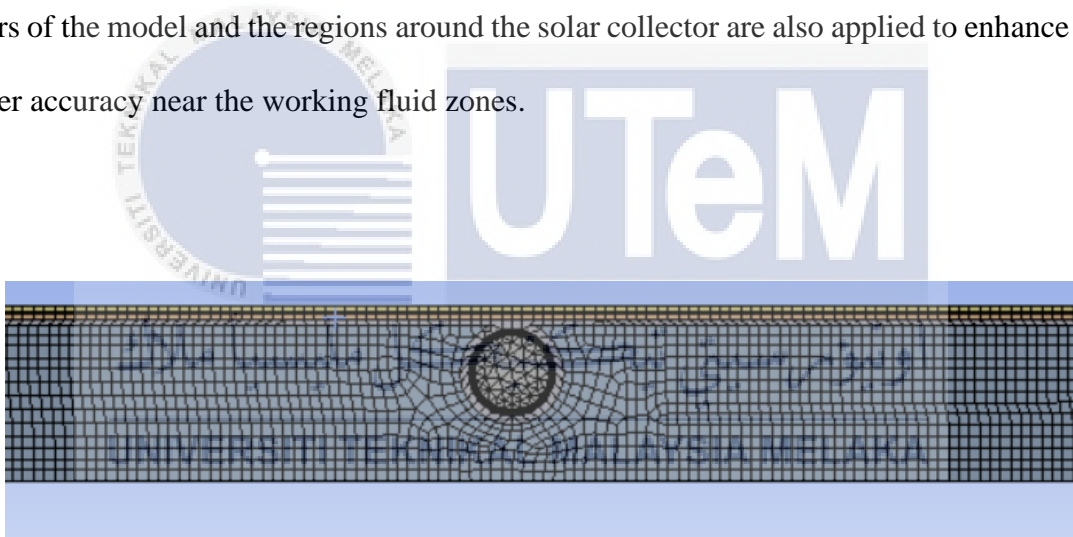


Figure 3.5 - meshing results produced in the present study.

The generated mesh is then checked to verify whether the quality of the mesh is acceptable to produce reliable results in ANSYS Fluent. From the ANSYS Meshing software, the reported average orthogonal quality of the meshed model with 3,335,771 nodes and 3,481,795 elements is 0.94 and the average skewness is 0.085. It can be concluded that the mesh quality of this model is acceptable and can be used for simulation in ANSYS Fluent software based on the ANSYS Mesh Quality recommendations. However, a mesh

independence study for this model is still needed ensure accurate results is produced from this model.

3.3.6.1 MESH INDEPENDENCE STUDY

Figure 3.5 illustrates the model's mesh distribution. As seen in this picture, ANSYS MESHING software was used to create a three-dimensional structural mesh. Near the collection walls, the grid is refined to analyse the change temperature gradients in these places. To optimise the accuracy and speed of numerical simulations, the results should be independent of mesh sizes. To accomplish this, a mesh independence study is conducted using four different mesh sizes in relation to water as the working fluid. Additionally, the base case conditions for this study are mentioned in Table 4.1.

Table 3.2 - mesh independence study for different mesh sizes.

Element size (m)	No. of elements	Average coolant outlet temperature (°C)
0.1	3,601,059	34.2832
0.2	3,481,795	34.2851
0.3	3,263,974	34.2974
0.4	3,197,717	34.3110

From Table 3.2, it can be seen that the difference between element sizes of 0.1 m and 0.2 m is the least compared to 0.3 m and 0.4 m element size. Hence, element size of 0.2 m is chosen for all of the simulations used in this study to reduce computational cost and simulation time.

3.4 THERMODYNAMIC ANALYSIS

Thermodynamic analysis is critical for evaluating the performance of various systems. Thermodynamic analysis is separated into two parts, which are energy and exergy analysis. In this study, the performance of PVT/PCM system are investigated based on energy analysis

The effective incident solar radiation, $\dot{E}_{eff,sun}$, to the system that can be expressed as:

$$\dot{E}_{eff,sun} = \tau_g \alpha_{cell} A_{PV} \dot{E}_{sun} \quad (3.13)$$

where, τ_g is the glass cover transmissivity, α_{cell} the cell absorptivity, A_{PV} is the area of PV unit and \dot{E}_{sun} is the overall incidence rate. The following equation is used to determine the electrical efficiency of PVT/PCM systems.

$$\eta_{el} = \frac{\dot{E}_{el}}{\dot{E}_{eff,sun}} = \eta_r \cdot [1 - 0.0045 \cdot (T_{cell} - 298.15)] \quad (3.14)$$

where, η_r and T_{cell} are the efficiency of the solar module under normal test conditions and the operating temperature of the photovoltaic cells, respectively. The PVT/PCM system's thermal energy efficiency is determined as follows:

$$\eta_{th} = \frac{\dot{m}_f \cdot C_{p,f} \cdot (T_{f,out} - T_{f,in}) + \dot{E}_{PCM}}{\dot{E}_{sun}} \quad (3.15)$$

where, $C_{p,f}$, $T_{f,in}$, $T_{f,out}$, and \dot{E}_{PCM} are mass flow rate, specific heat capacity, inlet and outlet temperatures of the collector's working fluid., and thermal power absorbed by PCM, respectively.

$$\dot{E}_{PCM} = \begin{cases} \frac{m_{PCM}C_{p,PCM}(T_{PCM,t}-T_{PCM,t_0})}{t-t_0} & t < t_1 \\ \frac{m_{PCM}C_{p,PCM}(T_{PCM,t_1}-T_{PCM,t_0})}{t_1-t_0} + \frac{m_{PCM}h}{t-t_1} & t_1 \leq t \leq t_2 \\ \frac{m_{PCM}C_{p,PCM}(T_{PCM,t}-T_{PCM,t_0})}{t-t_0} + \frac{m_{PCM}h}{t-t_1} + \frac{m_{PCM}C_{p,PCM}(T_{PCM,t}-T_{PCM,meting})}{t-t_2} & t > t_2 \end{cases} \quad (3.16)$$

where m_{PCM} are mass of PCM, $C_{p,PCM}$ is the specific heat capacity of PCM, h is the enthalpy of fusion of PCM, $T_{PCM,t}$, T_{PCM,t_1} , T_{PCM,t_0} are the temperature of PCM at time t , melting temperature and initial temperature of PCM, respectively. Furthermore, t_0 , t_1 , and t_2 is the initial time, time when PCM starts melting, and the time when PCM finishes melting process, correspondingly.



CHAPTER 4

RESULTS AND DISCUSSION

4.1 VALIDATION

The simulation results of this study are validated through the existing numerical study of the PVT/PCM system.

4.1.1 QUANTITATIVE VALIDATION RESULTS

The surface temperature contour of the PVT/PCM system is presented and compared. The temperature distribution in different sections of the PVT/PCM system is shown below. The comparison is made at the last time step of the simulation. The simulation setup of this validation is based on the base case conditions stated by (Kazemian, Salari, Hakkaki-Fard, & Ma , 2019). The base case of this validation is shown in Table 4.1.

Table 4.1 - Base case conditions (Kazemian, Salari, Hakkaki-Fard, & Ma , 2019).

Parameter	Base case condition
Absorbed solar radiation (W/m ²)	800
Wind speed (m/s)	1
Ambient temperature (°C)	30
Coolant inlet temperature (°C)	30
Coolant mass flow rate (kg/h)	30
Melting temperature of PCM (°C)	55
Enthalpy of fusion of PCM (°C)	170

Thermal conductivity of PCM (W/m.K)	0.25
Density of PCM (kg/m ³)	800
Specific heat capacity of PCM (J/kg.K)	2300

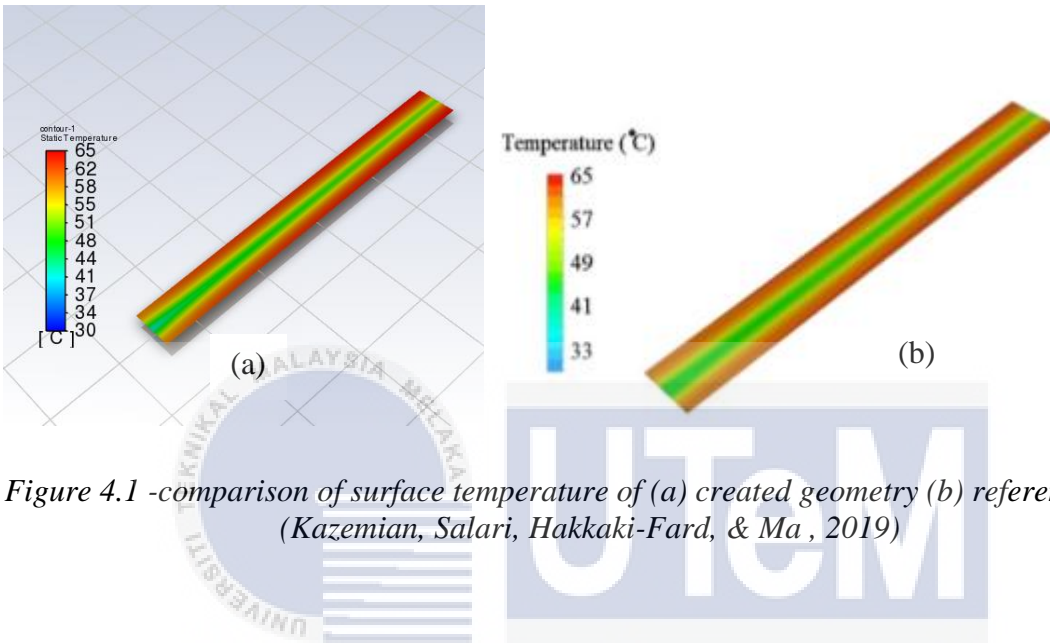


Figure 4.1 -comparison of surface temperature of (a) created geometry (b) reference paper (Kazemian, Salari, Hakkaki-Fard, & Ma , 2019)

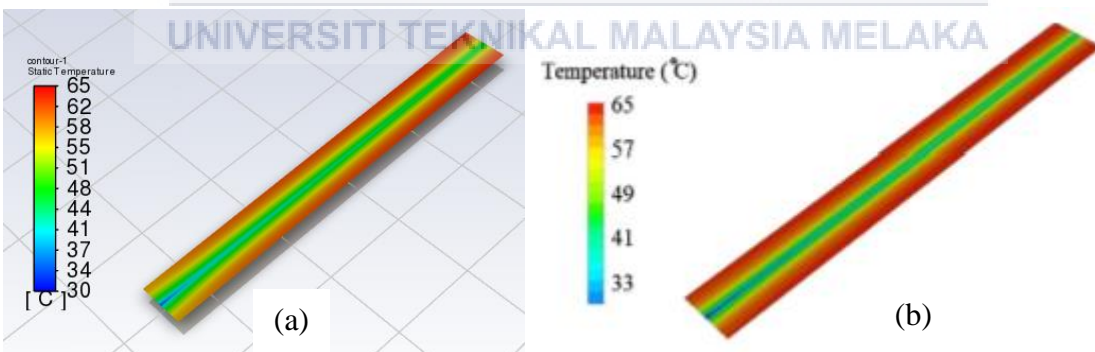


Figure 4.2 - PCM layer temperature comparison of (a) created geometry and (b) reference paper.

Based Figure 4.1, it can be seen that the minimum and maximum temperature of both created geometry and reference paper are the same, which is the maximum and minimum temperature contour are between 30 °C and 65 °C. The temperature contour around the

copper sheet and tube absorber has reduced temperature compared to other parts of the system. This is because, the water in the copper collector tube absorbs heat and hence, keeps the temperature around the collector at a low level compared to other parts of the system. Based on the simulation results, the average surface temperature obtained by referring to base case conditions for both created geometry and reference model for PVT/PCM system is 59.46 °C and 55.62 °C, respectively. The percentage difference of the surface temperature between the results obtained from the simulation and the numerical simulation by (Kazemian, Salari, Hakkaki-Fard, & Ma , 2019) is 6.90%. In addition, the percentage of melted PCM and the coolant outlet temperature is also compared and the percentage different between the current simulation results and numerical results of (Kazemian, Salari, Hakkaki-Fard, & Ma , 2019) is 6.49% and 8.49%, respectively. Quantitatively, there is a good agreement of this simulation study of the current simulation to the research that has been made on PVT/PCM system.

4.1.2 QUALITATIVE VALIDATION RESULTS

The comparison of simulation results of the melting temperature effect on the PCM is presented and compared. The simulation set up in this present study is using the same base case conditions as in Table 4.1. The results of average coolant outlet temperature, surface temperature of the PVT/PCM system, and the percentage of melted PCM is compared and presented below:

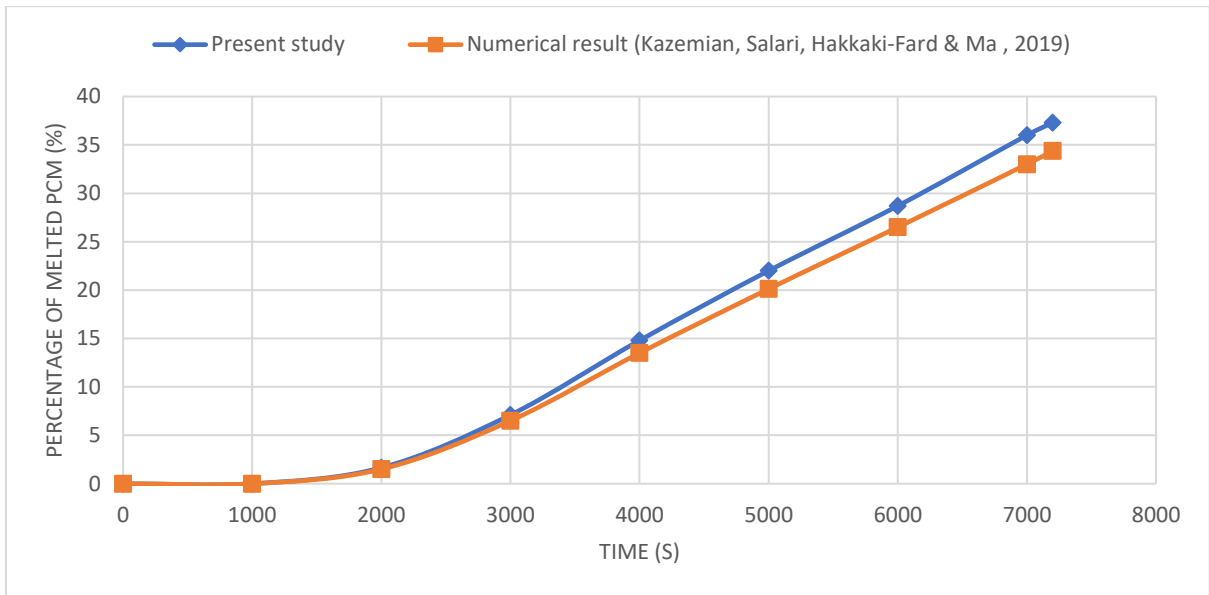


Figure 4.3 - Comparison of percentage of melted PCM between present study and numerical results of (Kazemian, Salari, Hakkaki-Fard, & Ma , 2019).

Based on Figure 4.3, the percentage of melted PCM of the present study and the numerical results of (Kazemian, Salari, Hakkaki-Fard, & Ma , 2019) at the last time step of the simulation is 37.3% and 34.37%, respectively. The maximum and average difference between current study and numerical results of (Kazemian, Salari, Hakkaki-Fard, & Ma , 2019) are also recorded. The maximum and average difference for this comparison is 9.63% and 7.07%, respectively.

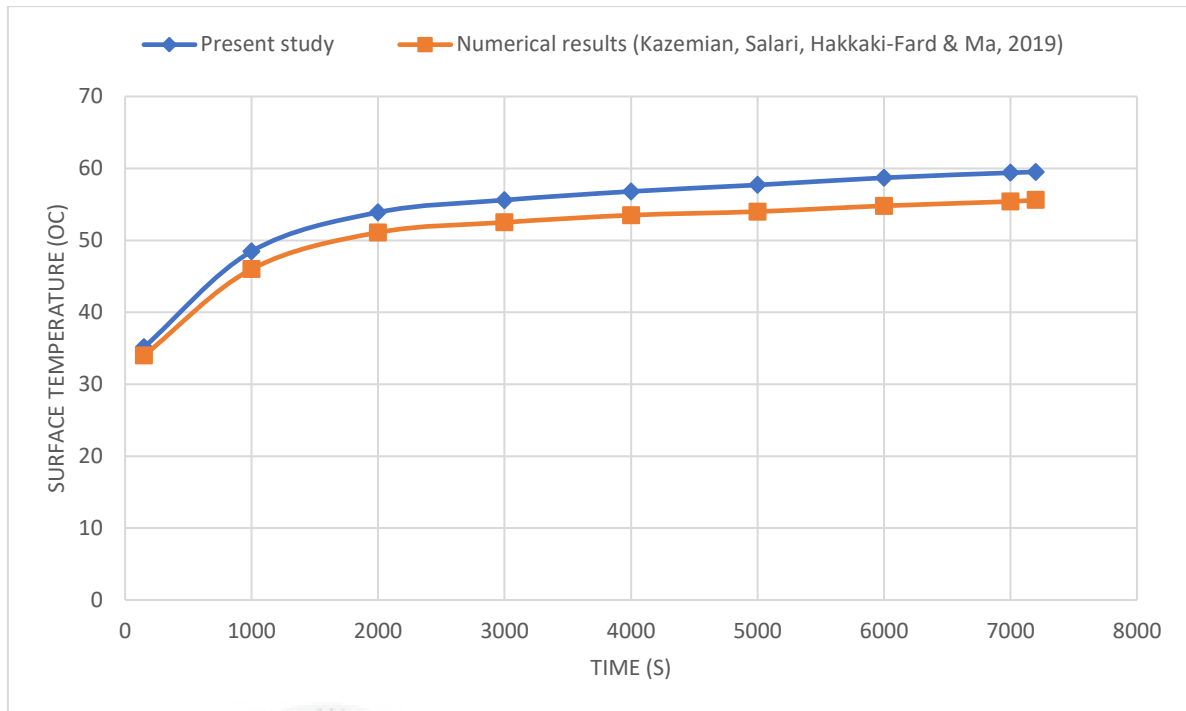


Figure 4.4 - Comparison of Average surface temperature of PVT/PCM system between present study and numerical results of (Kazemian, Salari, Hakkaki-Fard, & Ma , 2019).

Based on Figure 4.4, the recorded average surface temperature of the PVT/PCM system at the time step of 150, 1000, 2000, 3000, 4000, 5000, 6000, 7000, 7200 of both the present study and the numerical results of (Kazemian, Salari, Hakkaki-Fard, & Ma , 2019) are presented in Figure 4.4. From the Figure, it can be seen that the present study has a slightly higher temperature than the referred research paper. The maximum and average difference are also recorded. The maximum and average difference between current study and numerical results of (Kazemian, Salari, Hakkaki-Fard, & Ma , 2019) is 7.12% and 6.03%, respectively.

Based on Figure 4.5, the comparison between numerical results of (Kazemian, Salari, Hakkaki-Fard, & Ma , 2019) and current study is presented and recorded. The simulation setup of the recorded results is the same as the base case conditions represented in Table 4.1.

The maximum and average difference of the coolant outlet temperature presented in Figure 4.5 is 3.82% and 3.68%, respectively.

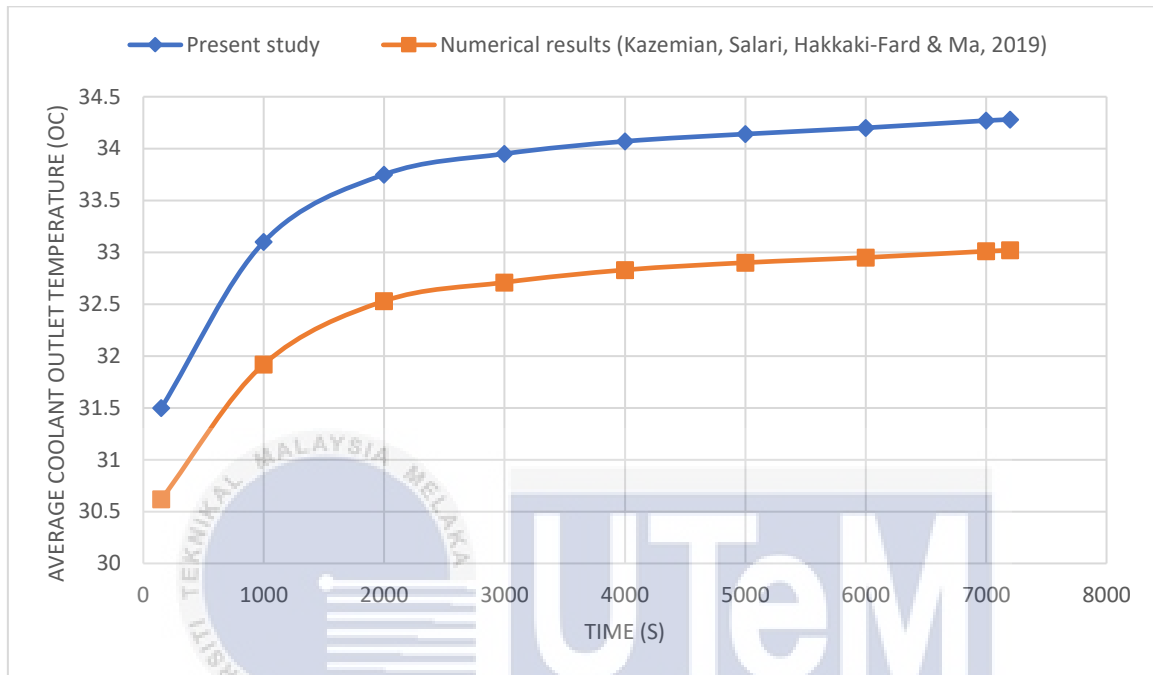


Figure 4.5 - Comparison of Average coolant outlet temperature between present study and numerical results of (Kazemian, Salari, Hakkaki-Fard, & Ma , 2019).

The comparison between the present study and the numerical results by (Kazemian, Salari, Hakkaki-Fard, & Ma , 2019) have been conducted and the percentage difference for both maximum and average difference are presented in Figure 4.3, 4.4, and 4.5. The maximum and average difference for the percentage of melted PCM, average surface temperature of PVT/PCM system, and coolant outlet temperature of the solar collector for the present study and numerical results of (Kazemian, Salari, Hakkaki-Fard, & Ma , 2019) is below 10% difference. Hence, there is a good agreement between the recent study and the referred research.

4.2 PROPOSED RESULT

The validated model of the PVT/PCM system will be improved by increasing the thickness of the PCM from 15 mm to 40 mm and changing the type of the PCM based on the commonly used PCM in Malaysia. The purpose of this study is to analyse the performance of the PVT/PCM system with increasing thickness of PCM and to improve the electrical and thermal efficiency of the existing model based on previous study.

4.2.1 SELECTION OF PCM

In this part, the selection of PCM is based on the solid-liquid PCM types that is commonly used in Malaysia. This is because, they have the advantage of low change in volume during phase transition process and have high latent heat capacity compared to liquid-gas PCM and solid-gas PCM (Lin, Jia, Alva, & Fang, 2017). Organic PCM has been chosen for this study as it possesses no toxicity, non-corrosive, has high chemical stability, melt congruently, high latent heat, recyclable, and is available at low cost. Both paraffin and non-paraffin type of PCM were chosen for the CFD simulation to investigate its performance to the PVT/PCM system. The selected PCM from the reference paper is also chosen for study to compare the performance of selected PCM used for study and the reference paper.

Furthermore, Paraffin A44 has been chosen for the organic paraffin type of PCM while Lauric acid has been chosen for the organic non-paraffin type of PCM. This is because, both Paraffin A44 and Lauric acid has suitable operating temperature for Malaysian weather conditions which shows that PV cell temperature can range from 25 °C to a little more than 70 °C in different weather conditions (Fayaz, Rahim, Hasanuzzaman, Rivai, & Nasrin, 2019). Therefore, a suitable PCM with melting temperature ranging around 40 °C to 45 °C at peak solar radiation is chosen to keep low PV cell temperature. The thermophysical properties of the PCM chosen for this study is presented in Table 4.2.

Table 4.2 - Selected PCM used for study.

Type of PCM	Reference	Paraffin A44	Lauric Acid
	paper (Kazemian, Salari, Hakkaki-Fard, & Ma , 2019)		
Density (kg/m³)	800	912	1007
Specific heat (J/kg. K)	2300	2400	1760
Thermal conductivity (W/m. K)	0.25	0.24	0.442
Viscosity (kg/ms)	0.0065	0.007	0.00688
Latent heat (kJ/kg)	170	250	211.6
Melting temperature (°C)	55	44	43.8

4.2.1.1 SIMULATION RESULTS OF USING DIFFERENT TYPES OF PCM

A simulation study is done using ANSYS FLUENT on the performance of the PVT/PCM system by using different types of PCM. The percentage of melted PCM, coolant outlet temperature, and the surface temperature of the PVT/PCM of all types of PCM has been recorded and presented.

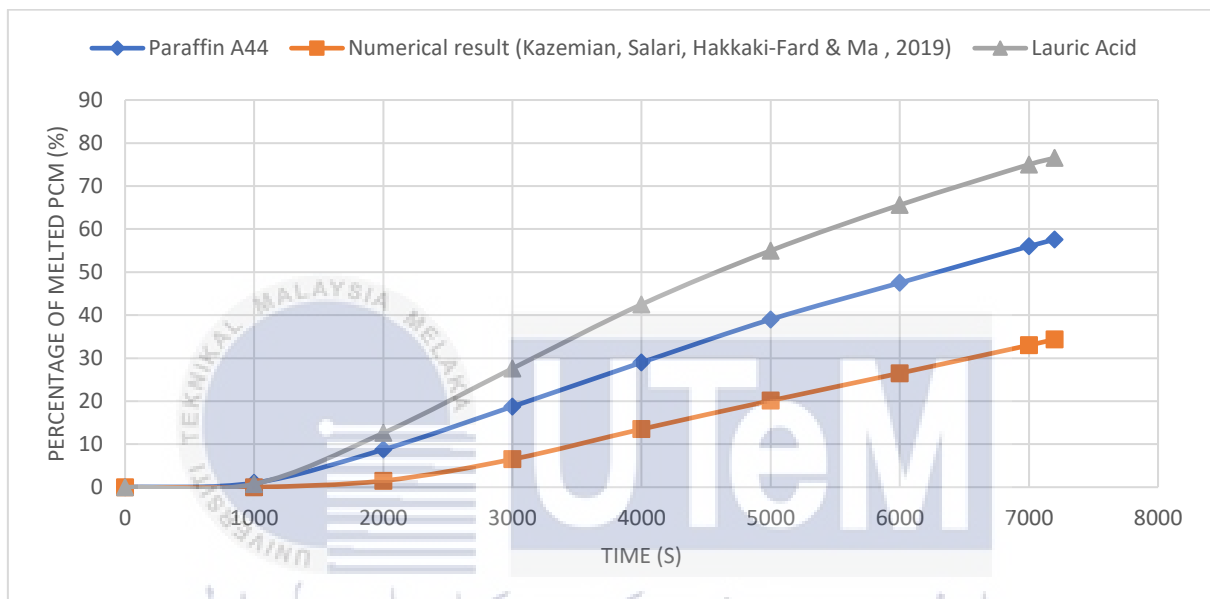


Figure 4.6 - Percentage of melted PCM for different types of PCM.

Based on Figure 4.6, Lauric Acid has the highest percentage of melted PCM followed by Paraffin A44 and the PCM used by the reference paper with all of them have the percentage of 76.53%, 57.54%, and 34.37%, respectively. Furthermore, the time taken for the PCM to start melting for the reference paper has been the longest compared to other PCMs. This is because, the melting temperature of PCM used by the reference paper is the highest a 55 °C compared to Lauric Acid with 43.8 °C and Paraffin A44 with 44 °C. As the melting temperature increases, the time taken for the PCM to melt increases. Hence, the

percentage of melted PCM at the last time step of the simulation will decrease as melting temperature increases.

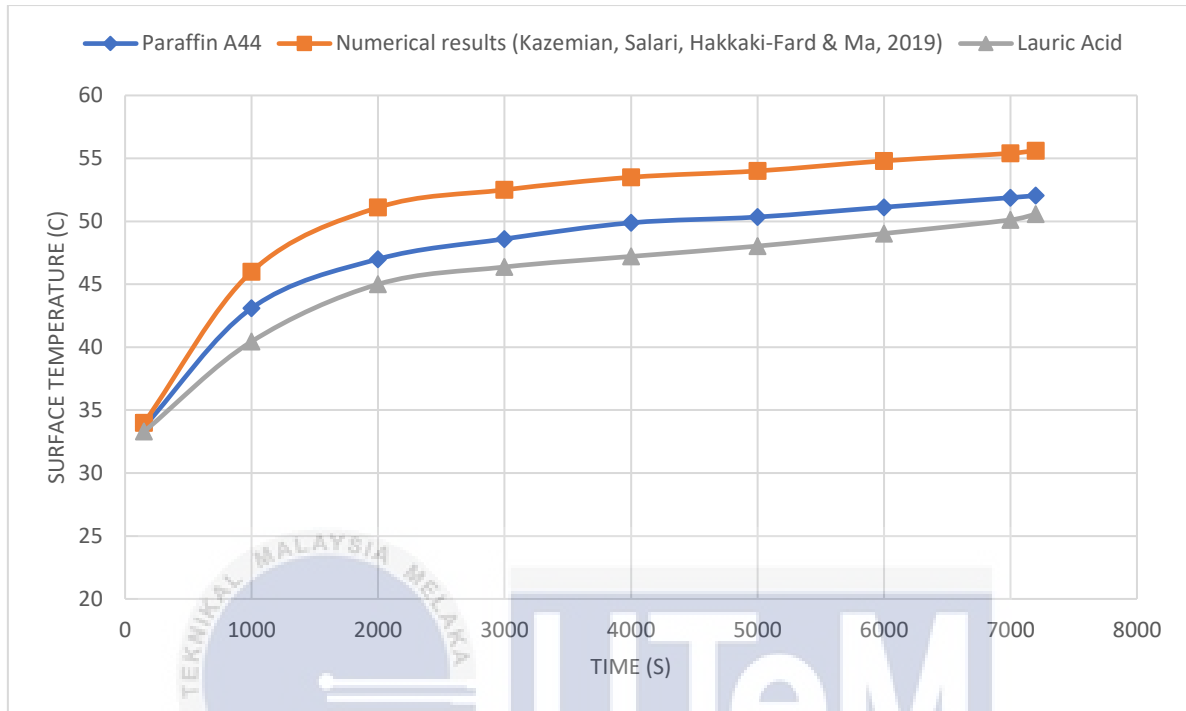


Figure 4.7 - surface temperature of different types of PCM.

The surface temperature of Lauric Acid is the lowest compared to other PCMs. From Figure 4.7, it can be seen that the curve for all PCMs is increasing gradually before it reaches specific temperature. This is because the PCM is still in solid phase and still not started melting. When it reaches temperature that is close to their melting temperature, the surface temperature will start to increase slowly as it is already in the transitional phase and the PCM is starting to melt. As the melting temperature of the PCM increases, the surface temperature of the PVT/PCM system also increases as it requires more heat to melt the PCM. It is also observed that the curve for Paraffin A44 is quicker to regulate the surface temperature compared to other PCMs. This is because, Paraffin A44 has the highest value of latent heat compared to Lauric acid and the PCM used in the reference paper. As a result, when latent

heat increases, more heat can be absorbed by PCM during the melting process, lowering the system's surface temperature.

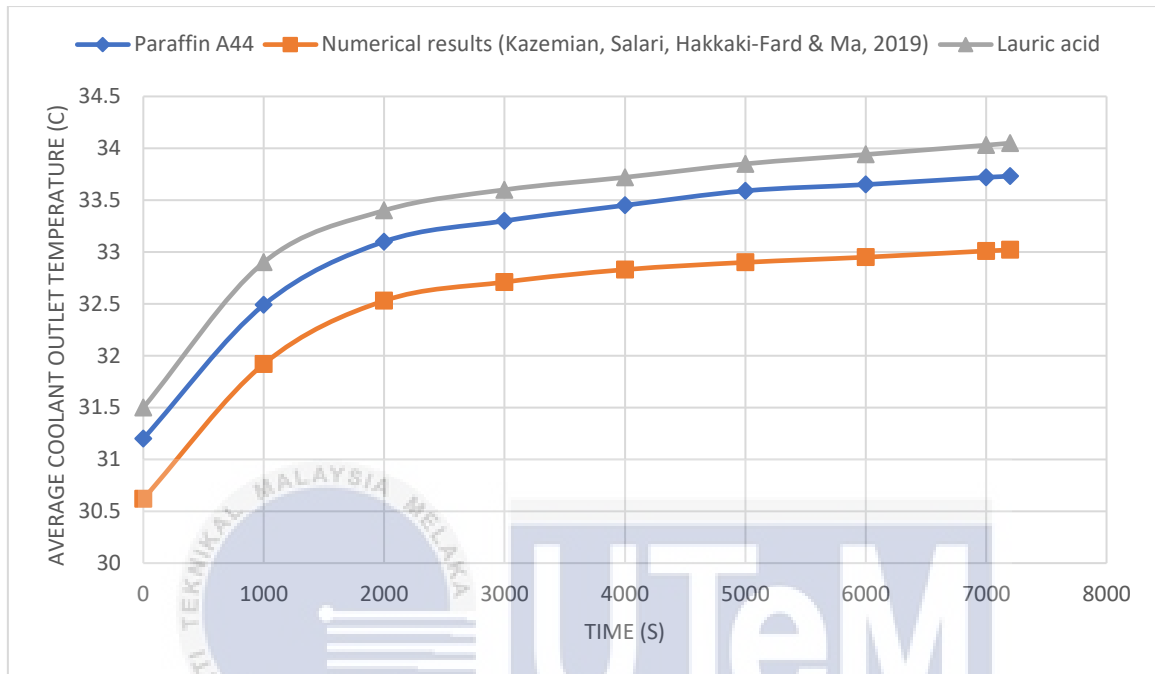


Figure 4.8 - Average coolant outlet temperature of different types of PCM.

Figure 4.8 shows the average coolant outlet temperature for different types of PCM. The coolant outlet temperature for Lauric Acid has been the highest at the last time step of the simulation compared to other PCMs. This is because, Lauric Acid has the highest thermal conductivity compared to PCM used by reference paper and Paraffin A44. This is because, increased thermal conductivity accelerates the heat storage and extraction processes associated with melting and solidification (Mesalhy, Lafdi, Elgafy, & Bowman, 2005). Increasing thermal conductivity will also increase coolant outlet temperature because of the energy absorption rate of PCM increases.

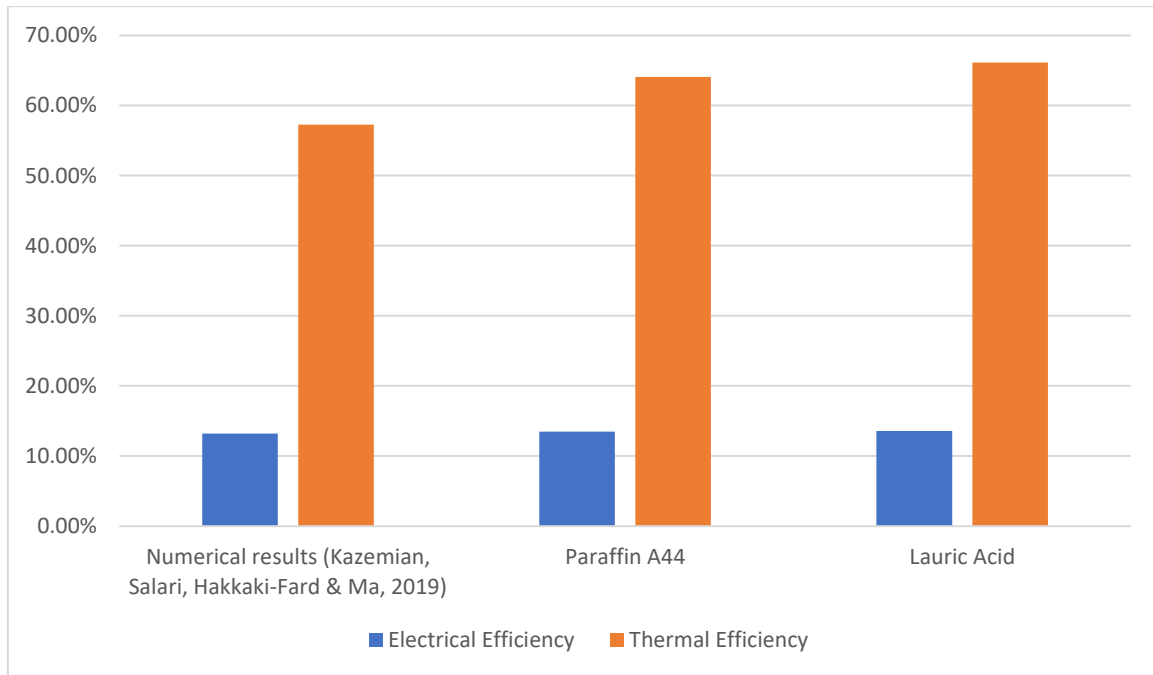


Figure 4.9 - Comparison of electrical and thermal efficiency of PVT/PCM system with different types of PCM.

The comparison of electrical and thermal efficiencies for different types of PCM can be seen in Figure 4.9. The electrical efficiency enhancement of using Lauric Acid can be increased to 13.57% from 13.22% when using the PCM from the numerical result while using Paraffin A44 can increase the electrical efficiency to 13.48%. the overall increment of electrical efficiency for Lauric Acid and Paraffin A44 compared to the reference paper is 2.65% and 1.97%, respectively.

For the thermal efficiency, Lauric Acid has the highest value which is 66.12% compared to Paraffin A44 and reference paper which has 64.07% and 57.30%, respectively. Using Lauric Acid can increase the thermal efficiency of the system by 15.39% while Paraffin A44 can increase by 11.81%.

It can be concluded that Lauric Acid has better overall performance compared to other PCMs as it has higher thermal conductivity, lower melting temperature, and high density and high latent heat.

4.2.2 SIMULATION STUDY OF USING DIFFERENT THICKNESS OF PCM

In this part, a simulation of using different thickness of PCM is studied and investigated to find the optimum thickness and improve the electrical and thermal efficiency of the PVT/PCM system. A selection of PCM thickness ranging from 15 mm to 50 mm has been chosen for this study. The selection of PCM thickness range is based on the properties of different types of PCM mentioned in Table 4.2. Other parameter used in this study is kept constant and is based on Table 4.1.

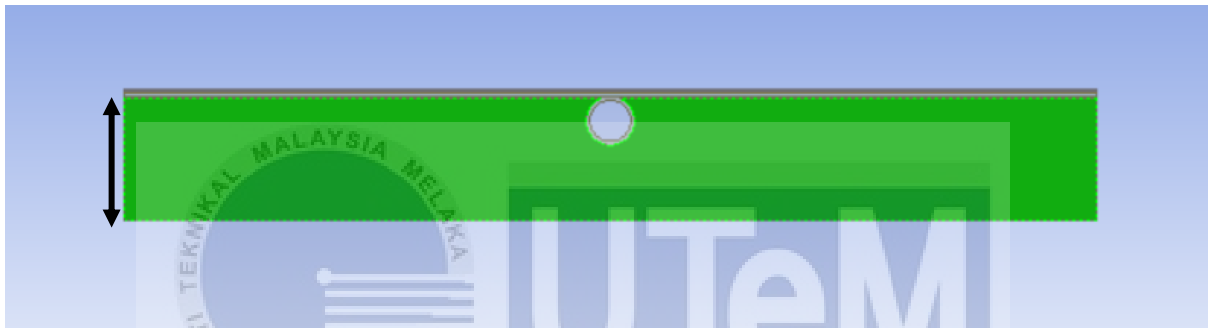


Figure 4.10 - thickness of PCM

4.2.2.1 SIMULATION RESULTS OF USING DIFFERENT THICKNESS OF PCM

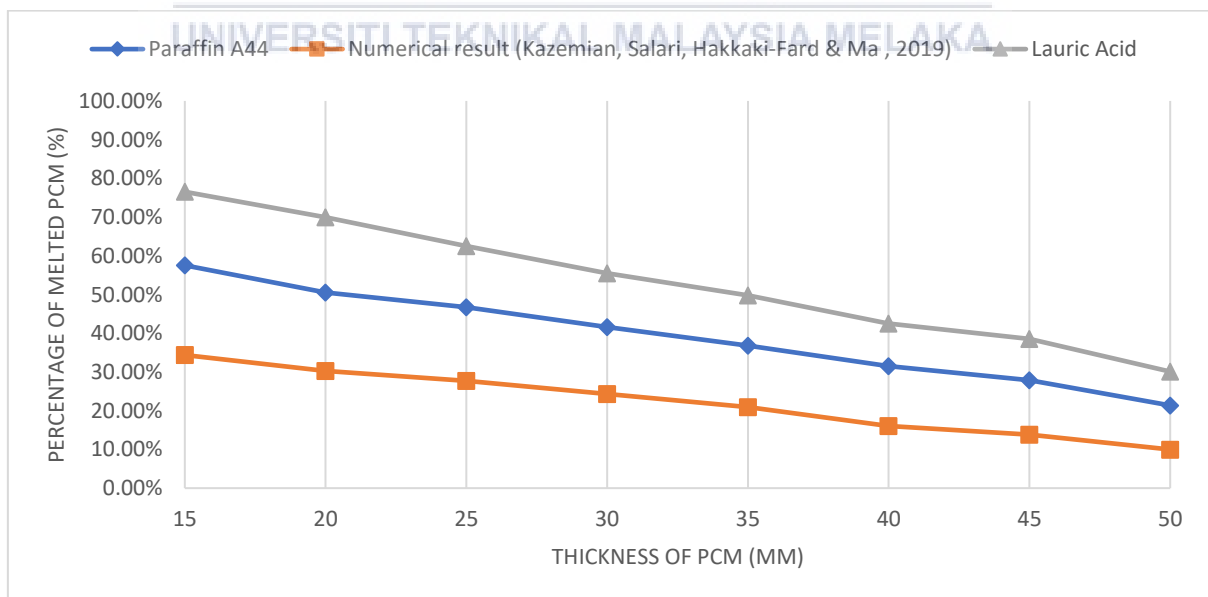


Figure 4.11 - percentage of melted PCM of different thickness.

The percentage of PCM of different thickness for different types of PCM is presented in Figure 4.11. Based on the simulation results, it can be observed that the percentage of melted PCM decreases for all PCMs as thickness increases. This is because, increasing the depth of the PCM also increases its mass and volume. As a result, the heat absorbed by the PCM cannot reach the bottom of PCM during melting phase. At 800 W/m² of solar radiation, Lauric Acid has the highest percentage melted at 50 mm thickness at 30.10% while the PCM used in the reference paper has the lowest percentage at 9.97%. However, having the lowest percentage of melted PCM at such high radiation can cause a lot of waste to the PCM in terms of economic and the performance of the system in the long run. This is because, solar radiation varies from time to time and at low radiation, the PCM may not be melted at all. Hence, selecting the thickness of the PCM at 25 to 30 mm is optimum for the system as it is still melted above 50% in case a higher radiation is received to the PV.

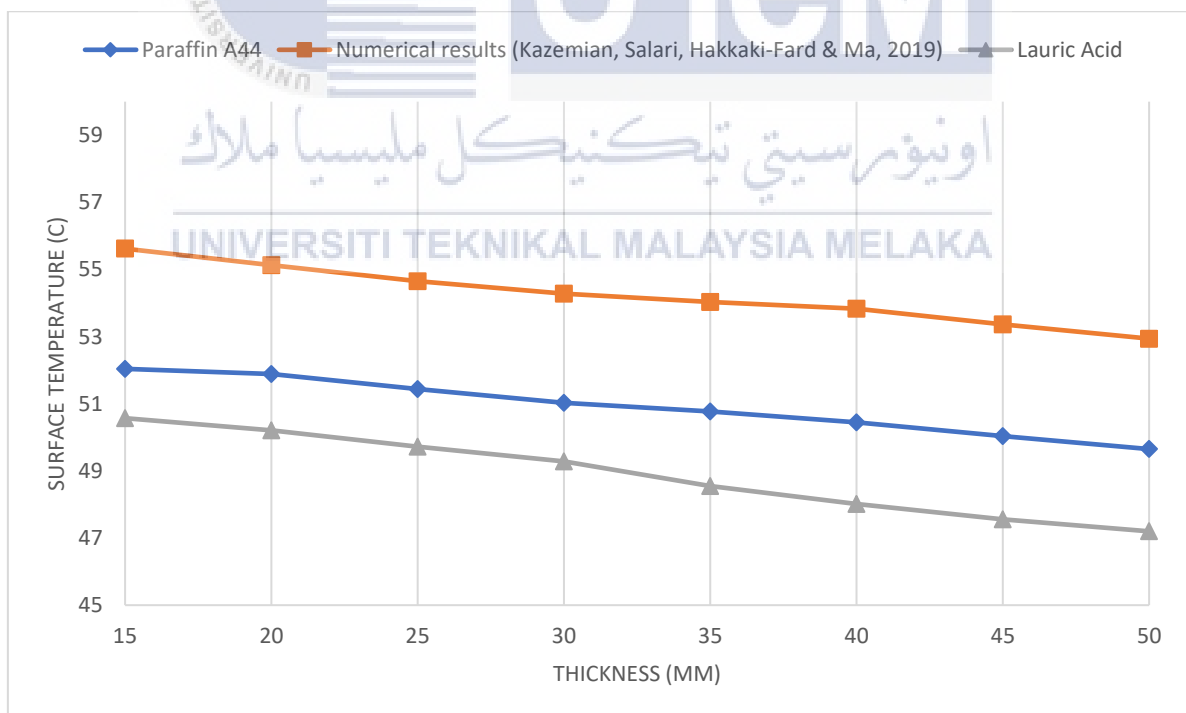


Figure 4.12 - surface temperature of PVT/PCM system using different thickness of PCM.

Based on Figure 4.12, the surface temperature of PVT/PCM system decreases for all types of PCM with increasing thickness of PCM. This is due to more heat is able to be absorbed during melting phase by the increasing volume of PCM. It can be observed that the reference paper has the highest surface temperature because it has the highest melting temperature compared to Lauric Acid and Paraffin A44. An optimum melting point can make the PCM reach maximum possible depth during phase changing process. Having too high or too low melting point makes the PCM spends too much time in either solid or liquid phase, hence reducing the efficiency of the system.

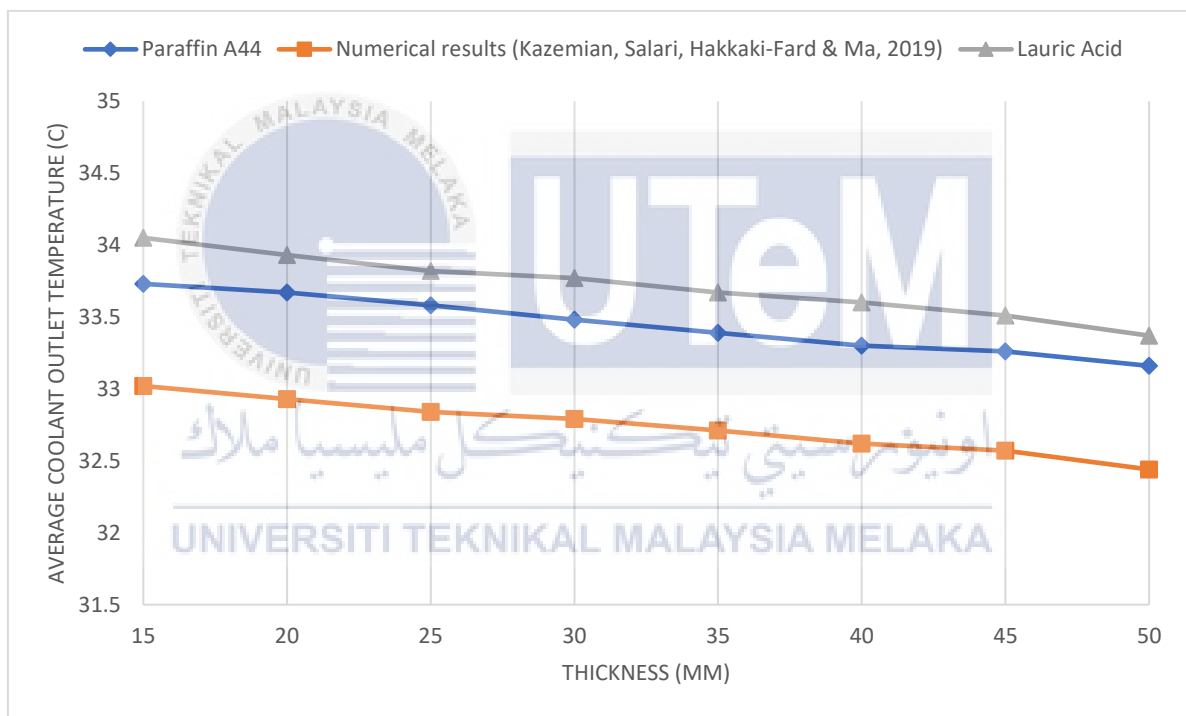


Figure 4.13 - average coolant outlet temperature for different thickness of PCM.

Based on the simulation results, it is observed that the average coolant outlet temperature is steadily decreasing as thickness of PCM increases. The results presented in Figure 4.13 shows that the temperature of Lauric Acid is the highest at 34.05 °C compared to Paraffin A44 and reference paper at 33.73 °C and 33.02 °C, respectively. At maximum thickness of 50 mm, the temperature of Lauric Acid, Paraffin A44 and the reference paper

at the last time step of the transient simulation are 33.37 °C, 33.16 °C, and 32.44 °C, respectively. It can be concluded that as the thickness of PCM increases the average coolant outlet temperature decreases due to the heat absorption by the PCM.

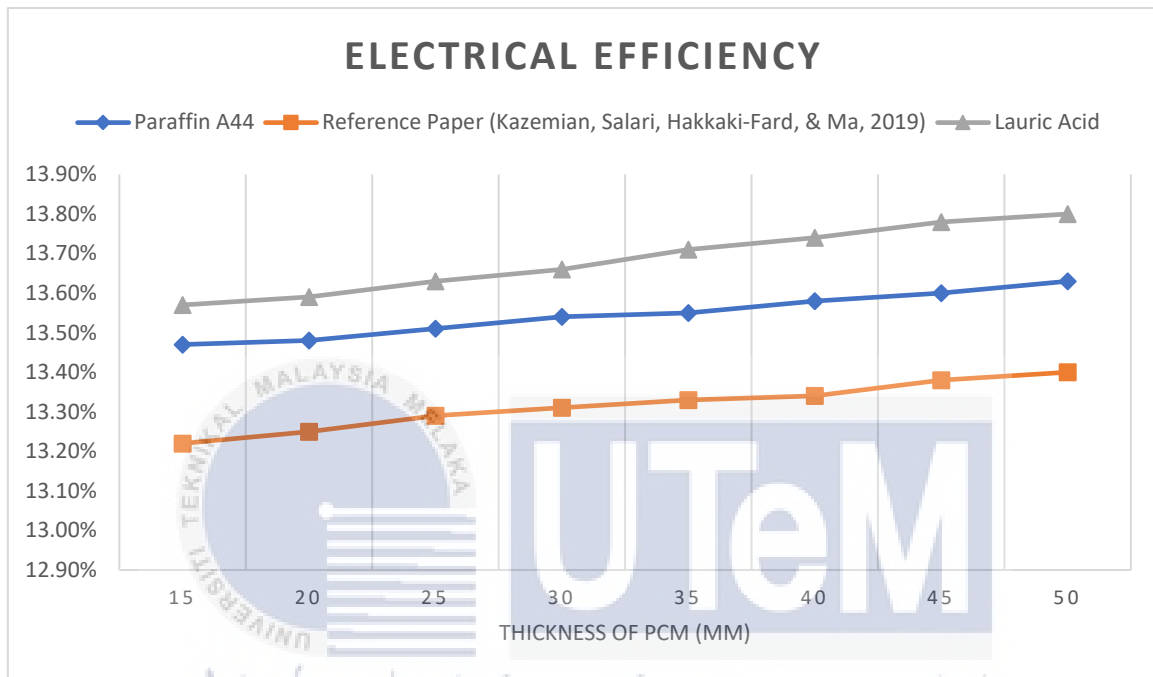


Figure 4.14 - Electrical efficiency of PVT/PCM system with different thickness.

The electrical efficiency of PVT/PCM with increasing thickness and calculated and presented as shown in Figure 4.14. From the results, it can be seen that the electrical efficiency of the reference paper is the lowest compared to Paraffin A44 and Lauric Acid. This is because, the surface temperature of the system is the highest for the reference paper, as a result of high melting temperature of the PCM. At PCM thickness of 50 mm, the reference paper has electrical efficiency of 13.40% while Paraffin A44 and Lauric acid has the electrical efficiency of 13.63% and 13.8%, respectively. It can be concluded that the PCM thickness increment enhances the electrical performance of the system.

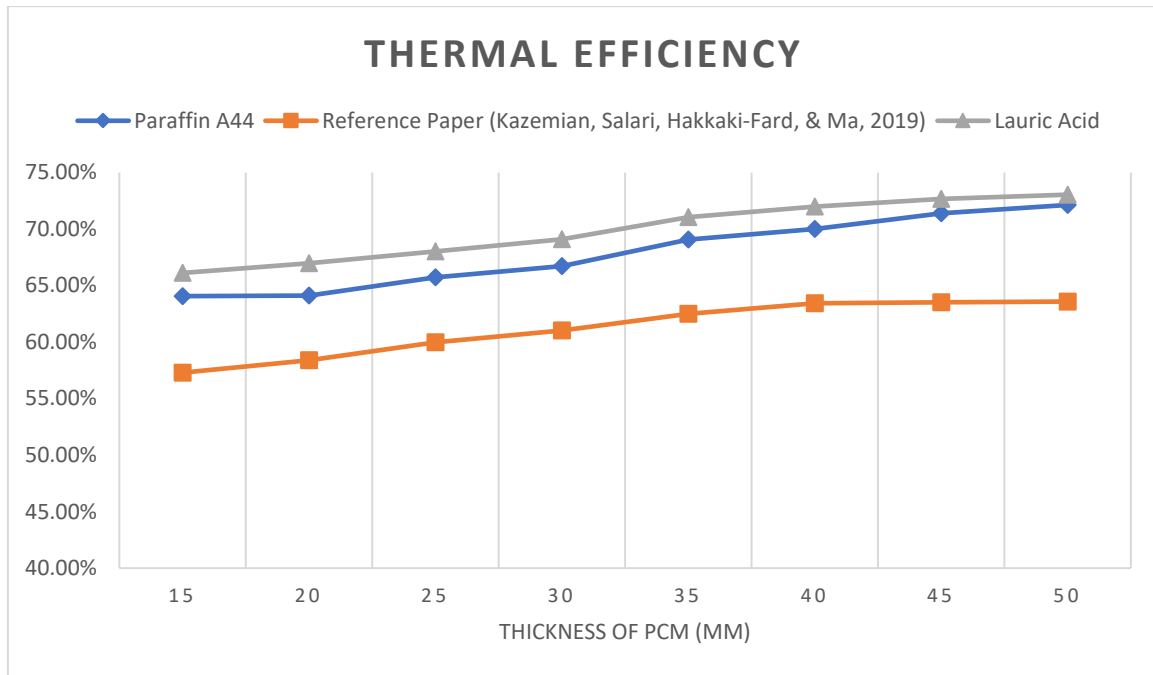


Figure 4.15 – Thermal efficiency of PVT/PCM system with different thickness

Based on Figure 4.15, it can be seen that the thermal efficiency of the PVT/PCM system increases as the thickness of PCM increases. Lauric Acid has the highest thermal efficiency compared to the reference paper and Paraffin A44. This is due to the increase in mass and volume of the PCM causes the time when PCM starts melting decreases. As a result, the PCM can absorb more thermal power thus increasing the thermal efficiency of the system. Lauric Acid has the shortest melting time among other PCMs for all levels of thickness, followed by Paraffin A44 and the reference paper, resulting in Lauric Acid highest thermal efficiency at 73.05% at thickness of 50 mm, while Paraffin A44 and the reference paper has 72.14% and 63.59%, respectively.

Overall, Lauric Acid is the optimal selection for this study at 30 mm thickness as it has the highest thermal and electrical efficiency, highest coolant outlet temperature, lowest surface temperature, and appropriate melting percentage among all other PCMs.

CHAPTER 5

CONCLUSION AND RECOMMENDATION FOR FUTURE WORK

5.1 CONCLUSION

The enhancement of thickness and changing to a different type of PCM that is suitable for Malaysian weather condition has been proven to increase both electrical and thermal efficiency of the PVT/PCM system. Paraffin A44 has high latent heat, which makes it easier to absorb heat per kilogram of PCM during melting process hence, reducing the temperature of the PV to improve electrical efficiency. However, lower thermal conductivity of Paraffin A44 makes it inefficient for the solar thermal system as the coolant outlet temperature is not high enough for solar thermal application. The high thermal conductivity in Lauric Acid improves the thermal and electrical efficiency of the system by 2.65% and 15.39%, respectively as the energy absorption rate of PCM is enhanced significantly compared to Paraffin A44. Besides, Lauric Acid also has the lowest melting point and high latent heat.

When it comes to the thickness of PCM, Lauric Acid has the best electrical and thermal efficiency at 30 mm thickness, valuing at 13.66% and 69.10%, respectively compared to other PCMs. Lauric Acid also has an appropriate melted percentage of PCM at specific radiation used for this simulation, highest coolant outlet temperature, and lowest surface temperature.

5.2 RECOMMENDATIONS FOR FUTURE WORK

Enhancing the design of the solar collector with the incorporation of fins in existing PVT/PCM can help utilizing the increasing thickness of the PCM. This is because, the incorporation of fins at the copper sheet and tube collector increases the surface area for heat transfer to the PCM. Furthermore, a proper height of fins can also utilize the maximum melting depth for the PCM during melting and solidification process. Moreover, the incorporation of using metal foam in PCM can also help enhance the thermal conductivity of the system and improving the temperature distribution inside the PCM.



REFERENCES

- A. , S., V.V., T., C.R., C., & D., B. (2009). Review on thermal energy storage with phase change materials and applications. *Renew. Sustain. Energy Rev.* 13, 318-345.
- Akeiber, H., Nejat, P., Majid, M., Wahid, M.A., Jomehzadeh, F., Zeynali, F., . . . Zaki, S. (2016). A review on phase change material (PCM) for sustainable passive cooling in building envelopes. *Renewable and Sustainable Energy Reviews*.
- Atal, A., Wang, Y., Harsha, M., & Sengupta, S. (2016). Effect of porosity of conducting matrix on a phase change energy storage device. *Heat and Mass Transfer*, 9-16.
- Badiee, Z., Eslami, M., & Jafarpur, K. (2019). Performance Improvements in Solar Flat Plate Collectors by Integrating with . *Energy*.
- Diwania, S., Agrawal, S., Siddiqui, S., & Singh , S. (2020). Photovoltaic–thermal (PV/T) technology: a comprehensive review . *International Journal of Energy and Environmental Engineering*.
- Essa, M., Talaat, M., Amer , A., & Farahat, M. (2021). Enhancing the photovoltaic system efficiency using porous metallic media integrated with phase change material. *Energy*.
- Fayaz, H., Rahim, N., Hasanuzzaman, M., Rivai, A., & Nasrin, R. (2019). Numerical and outdoor real time experimental investigation of performance of PCM based PVT system. *Solar Energy*.
- Huang, M., Eames, P., & Norton, B. (2004). Thermal regulation of building integrated photovoltaics using phase change materials. *Inernational Journal of Heat and Mass Transfer*.

- I., S., & A., D. (2019). Review on heat transfer analysis in thermal energy storage using latent heat storage systems and phase change materials. *Int. J. Energy Res.*, 29-64.
- Ibrahim, N., Al-Sulaiman, F., Rahman, S., Yilbas, B., & Sahin, A. (2017). Heat transfer enhancement of phase change materials for thermal energy storage applications: A critical review. *Renewable and Sustainable Energy Reviews*.
- Indartono, Y., Prakoso, S., Suwono, A., Zaini, I., & Fernaldi, B. (2015). Simulation and Experimental Study on Effect of Phase Change Material Thickness to Reduce Temperature of Photovoltaic Panel. *IOP Conference Series: Materials Science and Engineering*.
- Kazemian, A., Salari, A., Hakkaki-Fard, A., & Ma, T. (2019). Numerical investigation and parametric analysis of a photovoltaic thermal. *Applied Energy*, 734-746.
- Kenisarin, M., & Mahkamov, K. (2016). Passive thermal control in residential buildings using phase change materials. *Renewable and Sustainable Energy Reviews*.
- Khan, M., Saidur, R., & Al-Sulaiman, F. (2017). A review for phase change materials (PCMs) in solar absorption refrigeration systems. *Renewable and Sustainable Energy Reviews*.
- Lin, Y., Jia, Y., Alva, G. R., & Fang, G. (2017). Review on thermal conductivity enhancement, thermal properties and applications of phase change materials in thermal energy storage. *Renewable and Sustainable Energy Reviews*.
- Malvi, C., Dixon-Hardy, D., & Crook, R. (2011). Energy balance model of combined photovoltaic solar-thermal system incorporating phase change material. *Solar Energy* 85, 1440-1446.

- Mesalhy, O., Lafdi, K., Elgafy, A., & Bowman, K. (2005). Numerical study for enhancing the thermal conductivity of phase change material (PCM) storage using high thermal conductivity porous matrix. *Energy Conversion Management*.
- Mousavi, S., Kasaeian, A., Behshad Shafii, M., & Hossein Jahangir, M. (2018). Numerical investigation of the effects of a copper foam filled with phase. *Energy Conversion and Management*, 187-195.
- Reji Kumar, R., Samykano, M., Pandey, A., Kadirgama, K., & Tyagi, V. (2020). Phase change materials and nano-enhanced phase change materials for thermal energy storage in photovoltaic thermal systems: A futuristic approach and its technical challenges. *Renewable and Sustainable Energy Reviews*.
- Sathe, T., & Dhoble, A. (2019). Thermal analysis of an inclined heat sink with finned PCM container for solar applications. *International Journal of Heat and Mass Transfer*.
- Su, D., Jia, Y., Alva, G., Liu, L., & Fang, G. (2017). Comparative analyses on dynamic performances of photovoltaic–. *Energy Conversion and Management*, 79-89.
- Su, D., Jia, Y., Lin, Y., & Fang, G. (2017). Maximizing the energy output of a photovoltaic–thermal solar. *Energy and Buildings*, 382-391.
- Wang, T., Wang, S., Luo, R., Zhu, C., Akiyama, T., & Zhang, Z. (2015). Applications of solar water heating system with phase change material. *Renewable and Sustainable Energy Reviews*.
- Waqas Adeel, & Ji, J. (2017). Thermal management of conventional PV panel using PCM with movable shutters - a numerical study. *Solar Energy*.

- Yang, T., King, W., & Miljkovic, N. (2021). Phase change material-based thermal energy storage. *Cell Reports Physical Science*.
- Yuan, K., Shi, J., Aftab, W., Qin, M., Usman, A., Zhou, F., . . . Zou, R. (2019). Engineering the Thermal Conductivity of Functional Phase-Change Materials for Heat Energy Conversion, Storage, and Utilization. *Advanced Functional Materials*.
- Yuan, W., Ji, J., Modjinou, M., Zhou, F., Li, Z., Song Zhiying, . . . Zhao, X. (2018). Numerical simulation and experimental validation of the solar photovoltaic/. *Applied Energy*.

